Recommendations for enhancement of CHLA QC Methods

Ref.: D4.2_V1.0

Date: 15/12/2021

Euro-Argo Research Infrastructure Sustainability and Enhancement Project (EA RISE Project) - 824131

This project has received funding from the European Union's Horizon 2020 research and innovation programme under grant agreement no 824131.
Call INFRADEV-03-2018-2019: Individual support to ESFRI and other world-class research infrastructures

Disclaimer:

This Deliverable reflects only the author's views and the European Commission is not responsible for any use that may be made of the information contained therein.

Document Reference

Project	**Euro-Argo RISE - 824131**
Deliverable number	D4.2
Deliverable title	**Recommendations for enhancement of CHLA QC Methods**
Description	RT and DM procedures for CHLA concentration
Work Package number	WP4
Work Package title	Extension to Biogeochemical parameters
Lead Institute	Sorbonne Université
Lead authors	Catherine Schmechtig
Contributors	Fabrizio D'Ortenzio, Quentin Jutard, Raphaëlle Sauzède, P. R. Renosh, A. Poteau, H. Claustre, Marine Bretagnon, Antoine Mangin
Submission date	15/12/2021
Due date	[M36] - 31/12/2021
Comments	
Accepted by	Fabrizio D'Ortenzio

Document History

Version	Issue Date	Author	Comments
V1.0	15/12/21	Catherine Schmechtig	

EXECUTIVE SUMMARY

This deliverable presents the enhancements on quality control procedures performed on the CHLA concentration. The CHLA concentration is one of the six core variables of the BGC-Argo program. Regarding Real Time quality control procedures (already in place in several DACS), the main outcome relies on the improvement/correction of the existing procedures in place since 2014. Regarding Delayed Mode Quality control, the document presents how existing methods are applied to floats equipped with fluorometers and radiometers and an innovative method (machine learning method) to assess the correction for floats without radiometer. The different methods are widely tested and several ways to validate the results are reported.

TABLE OF CONTENT

1 Introduction

Right after the dissolved oxygen concentration, chlorophyll-a concentration (CHLA) has been one of the first variables implemented on BGC-Argo. Presently (december 2021), 212 floats equipped with a fluorometer are operational (see Figure 1), and approximately 90000 CHLA profiles have been acquired by BGC-Argo since the beginning of the program (Figure 2).

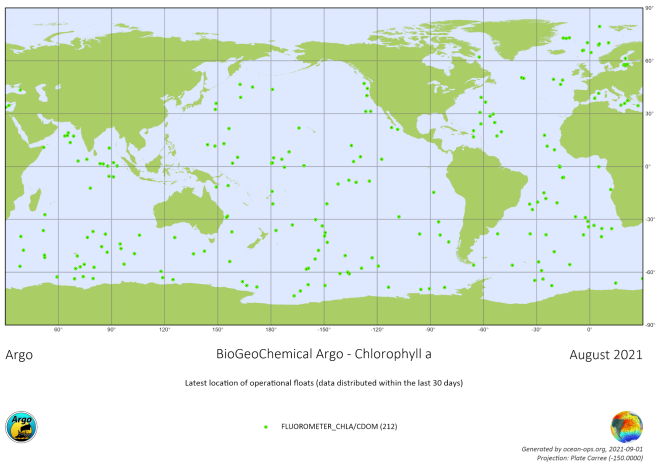

Figure 1: Active floats with fluorometers in August 2021 (https://www.jcommops.org/board)

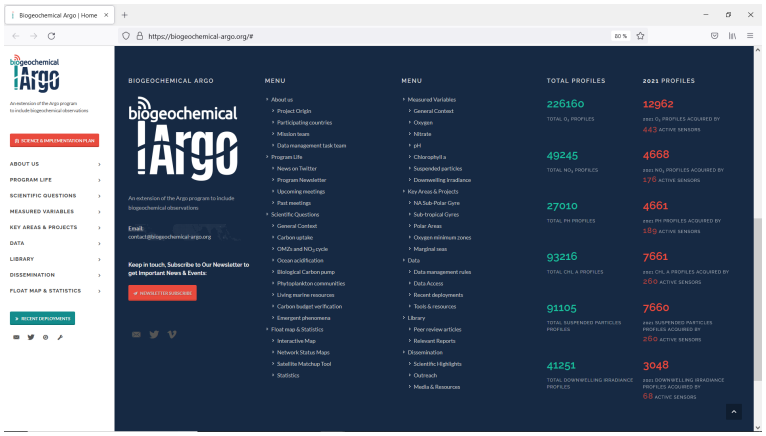

Figure 2: Total Chlorophyll-A profiles in Argo and profiles of Chlorophyll-A (93216) and since the beginning of 2021 (7661) (https://biogeochemical-argo.org/#) (2021/09/07)

The most used method to evaluate the CHLA parameter on floats is based on active fluorescence. Very roughly (for more details see Schmechtig et al., 2015), a fluorescence sensor excites a water volume with a blue light, measuring then the re-emitted light in the red portion of the spectrum. The emitted light is assumed to be proportional to the CHLA present in the water sample. The equation is :

$$CHLA = (FLUORESCENCE\_CHLA - DARK\_CHLA) * SLOPE\_CHLA \quad \text{Eq.1}$$

Where

CHLA = concentration of chlorophyll-a of a sample of interest (mg/m^3)

FLUORESCENCE_CHLA = raw counts output when measuring a sample of interest

DARK_CHLA = dark counts, the measured signal output of the fluorometer in clean water with black tape over the detector

SLOPE_CHLA = multiplier in mg/m^3/counts

The CHLA estimation from fluorescence is influenced by the physiological state of phytoplankton. It results in a variability of the fluorescence/chlorophyll ratio which can increase errors on the estimation from float. Moreover, the initial calibration (DARK_CHLA, SLOPE_CHLA) and the eventual long-term degradation of sensors may also impact the performance of the CHLA evaluation.

The first version of the BGC-Argo quality control manual for Chlorophyll-A concentration http://dx.doi.org/10.13155/35385 was released in 2014. Though the different assumptions and issues have been widely studied and tested there is still room to improve the quality control and adjustment for this parameter.

Presently, and after years of tests and developments (for the most conducted in the framework of international collaborations), the main issues of fluorescence-based CHLA estimation have been consensually identified :

1. Identification of bad points based on Argo common tests (range, spike…)
2. Adjustment procedures regarding:
    a. STEP1 : DARK CORRECTION (Estimation of DARK_CHLA, Eq. 1)
    b. STEP2: NON PHOTOCHEMICAL QUENCHING CORRECTION
    c. STEP3:SLOPE CORRECTION (Estimation of SLOPE_CHLA, Eq. 1)

The accepted quality control and adjustment strategy implies an estimation of the correct calibration factors (DARK_CHLA, SLOPE_CHLA) and the correction of the Non Photochemical Quenching effect both in Real Time (RT) and in Delayed Mode (DM). In Real Time, we assume to estimate these corrections using a standalone CHLA profile and T/S concurrent profiles. In Delayed Mode, we consider concurrent profiles (BBP, radiometry when available), other CHLA profiles acquired during the whole float life and ancillary data (i.e. remote sensing) to infer additional information.

The main objective of EA-RISE 4.2.1 task is to significatively progress in the development and tests of DM methods. The present document summarizes the EA-RISE effort for the DM for CHLA, and it will constitute the proposition of most of the EU players to the Argo international committees.

2 Real Time Quality Control

At GDAC level the RT Quality Control (RTQC) processing is currently implemented and operational. Its flowchart is presented in Figure 3 and the details of the algorithms could be found in the QC manual (http://dx.doi.org/10.13155/35385).

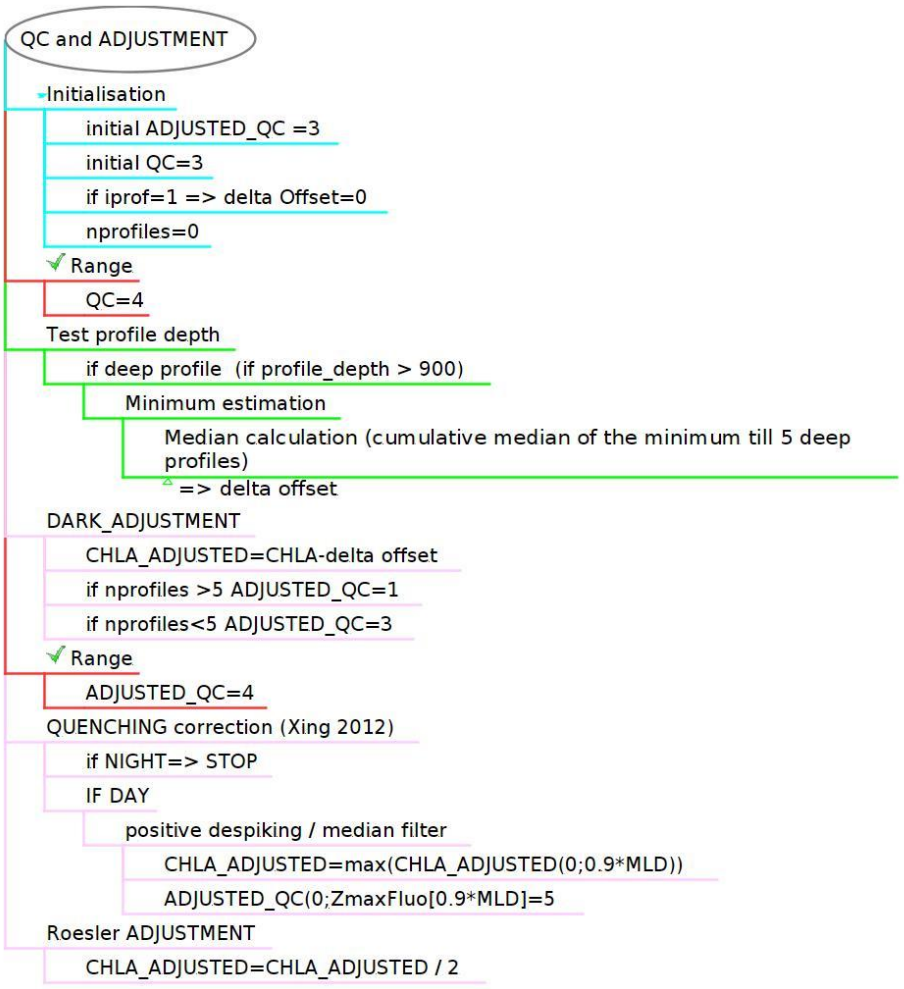

Figure 3: Flowchart of the RTQC and Adjustment for CHLA (2021)

While first released in 2014, the documentation of the quality control procedure for CHLA has been slightly revised in 2018. Some modifications have been introduced recently (regarding spikes detection and dark estimation). These modifications, agreed at ADMT, will be reported in the documentation. Associated tests and results are reported in the Annexes.

3 Delayed Mode Quality Control

At the beginning of the EA-RISE project, the DM QC for CHLA was still not implemented. This was the consequence of a lack of established methods. In this section, a first complete and consistent processor for DM is presented.

The processor is based on several R&D improvements performed and tested in the framework of EA-RISE. Operational implementation (i.e. development of shared tools, statistics, application to GDAC etc.) was also analysed during EA-RISE, on the basis of the proposed processor. Consequently, we separate the section in two sub-sections:

- "R&D", where the proposed methods are detailed, giving also information and references (if existing) and furnishing tests performed to evaluate the impact on existing profiles.
- "Operational", where the procedures to implement the proposed methods at operational level are presented.

3.1 General Overview

The proposed DMQC processor for CHLA parameter is based on 3 main steps, followed by a presentation of different ways to validate the results:

- STEP1 : DARK correction
- STEP2 : NON PHOTOCHEMICAL QUENCHING correction
- STEP3 : SLOPE correction
- VALIDATION

The proposed methods (which will be detailed in the next sections) required some external data and it massively uses a time-series of floats parameters. They minimize the scientific expertise required to perform the DM calculation, although a final validation from an expert is strongly recommended.

3.2 R&D

3.2.1 DARK CORRECTION

3.2.1.1 General introduction on the main philosophy

The DARK CORRECTION algorithm re-calculates the offset value, which is then applied to the fluorescence profile. This value is assumed to be the reference returned by the fluorometer in absence of chlorophyll-a, this value is then used as a 0 for the chlorophyll conversion. It could also change during the life of a float to account for sensor drift. In RTQC, the offset value was initially estimated from deep CHLA measurements (see Appendix 5.1 for detailed study) and is now estimated from the minimum of the profile. In DMQC, the DARK CORRECTION applied is then tested and verified, by recalculating the offset, not profile by profile, but with the information from the entire life of the float.

The method is based on Xing et al. (2011, 2014, 2017), using the results of Wojtasiewicz et al. 2018). It will be referred as “Median” method. It is conceptually similar to the approach used in the RT processing (i.e. searching CHLA values at depth assumed to be zero) with the notable difference that the whole data set of each float is scanned. In the DM processing, then, all the available profiles are used to provide a dark offset value. In this way, the final value is supposed to be more stable and less subject to overcorrection.

3.2.1.2 Implementation

The “Median” method is described in the following steps. For each float, the following operations are performed :

- Exclusion of profiles that do not have CHLA values deeper than 800 decibars.
- Filtering each profile with a centered running median on 5 values.
- Finding the minima of the filtered profiles (Xing et al. 2011 ; Xing et al. 2017 ; Wojtasiewicz et al. 2018).
- Computing the median of the minima (Xing et al. 2014).

3.2.1.3 Results

To evaluate the “Median” method, it was compared with the initial RTQC results. Tests were performed on a subset of profiles matching the following criteria :

- not on the greylist
- not from floats 3901036 and 3901037 (very poor data but not on the greylist)
- not in the Black Sea (these profiles do not reach low CHLA levels at depth)

The two methods give similar results (see Figure 4), although the “Median” method has a slightly lower Dark Offset value. The profiles showing the highest differences (values of the differences outside of range [−0.02 ; 0.05] mg/m3) are further analyzed.

The negative (i.e. values of Dark Offset from “Median” greater than those from “RTQC”) outliers (1534 profiles) correspond for the most part (1458 of them) to profiles collected when the RTQC method did not find a satisfying value. For this case, the RTQC Dark Offset values were defaulted to the factory value (which equal to 0). The remaining negative outliers (76 profiles) are mostly composed of bad data.

The positive (i.e. values of Dark Offset from “Median” lower than those from “RTQC”) outliers (182 profiles) are largely attributed to bad data (148 of them).

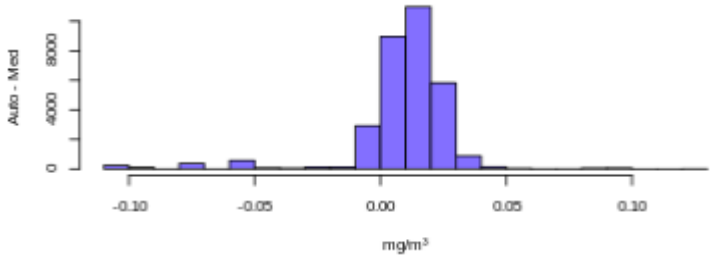

Figure 4 : Histogram of the difference between the RTQC (2014) computed dark offsets (Auto) and the median method (Med)

In summary, the median method provides dark offset values that are generally consistent with previous work on the RTQC although slightly lower. Considering the trend of the RTQC initial method for overcorrection (see appendix 5.1), the general trend of the median method is satisfactory, leading to less negative values below the Deep Chlorophyll Maximum (DCM). Additionally, based on a stronger statistic through the whole float life, the Median method looks robust.

In conclusion, the "Median" method is proposed to estimate the dark offsets in the delayed mode quality control of CHLA. In operational DM, we also propose to use a large running median filter when sensor drift is present.

3.2.2 NON PHOTOCHEMICAL QUENCHING CORRECTION

3.2.1.1 General introduction on the main philosophy

CHLA quality control requires compensation for non photochemical quenching (NPQ). The current correction of the NPQ in Real Time (Schmechtig et al., 2018) is based on the correction presented in Xing et al., (2012). It is particularly adapted to RT, being a standalone method not requiring ancillary data. Alternatives and more sophisticated NPQ corrections, however, have been recently proposed in the literature. For example, estimation of underwater light intensities, with subsequent NPQ correction above a certain light threshold only (Xing et al., 2018); multiple NPQ corrections based on the ratio between fluorescence and backscatter (e.g., Sackmann et al., 2008, Swart et al., 2015, Thomalla et al., 2018, Terrats et al., 2020) are more dedicated to DM procedures (while other Argo parameters (BBP, irradiances) are required as inputs) and were tested in the framework of EA-RISE. Based on results for more than 100 floats, this latest result (Terrats et al., 2020) gives really improved results on the correction of fluorescence in areas with low surface CHLA concentrations.

3.2.1.2 Implementation : Terrats et al., 2020

Terrats et al., 2020 show that the Xing et al., 2018 correction, for shallow mixing cases, could retrieve surface CHLA that differs from the night measurements by more than 200 %. They suggest an adapted NPQ correction as follows:

- For deep mixing cases (MLD > ipar_15)

  NPQ is corrected by multiplying BBP700 with the maximum of the CHLA/BBP700 ratio determined inside the mixed layer, (no deeper than ipar_15 if available). This method

originating from Sackmann et al., (2008) assumes uniformity in particle composition inside the mixed layer.

- For shallow mixing cases (MLD < ipar_15)

  Below MLD, NPQ is corrected with the sigmoid function of the Xing et al., 2018 method and the corrected ratio of CHLA/BBP700 at MLD is computed.

  Above MLD, we multiplied BBP700 by the CHLA/BBP700[MLD], assuming a constant CHLA/BBP700 ratio inside the remaining upper part of the mixed layer.

- Floats without radiometer and BBP sensor.

  In this case, the Xing et al., 2012 method is used.

3.2.1.3 Results

The Terrats et a., 2020 approach is tested on different cases (deep mixing case, shallow mixing case), considering whether or not the light. The presented figures have been performed for a float (6901493) equipped with the "best" sensor configuration which is a Fluorometer, a BBP sensor and a radiometer. The different cases, deep mixing and shallow mixing, are illustrated on the same profile with (Figure 5 and Figure 6) and without (Figure 7 and Figure 8) considering the light input, to highlight its influence on the result of the correction.

deep mixing cases (MLD > ipar_15)

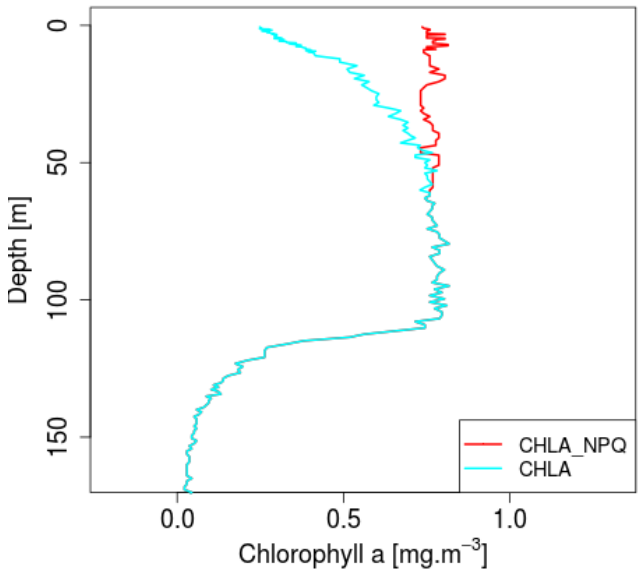

Figure 5 : Example of NPQ correction in deep mixing case profile 40, **float 6901493** MLD=113.6m, ipar_15=60.2m

shallow mixing cases (MLD < ipar_15)

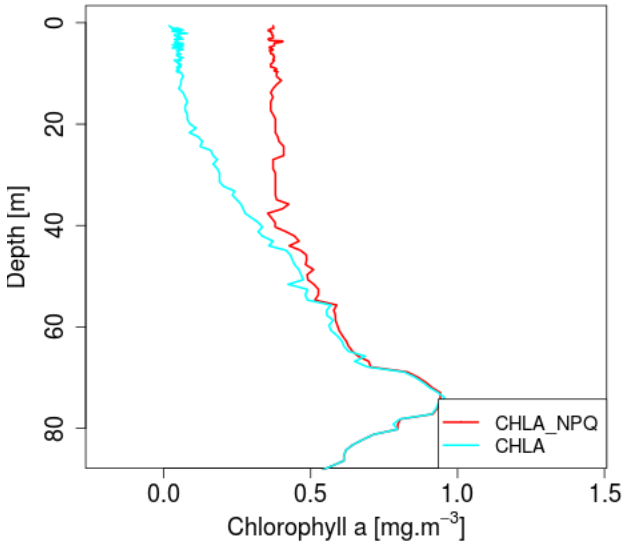

Figure 6: Example of NPQ correction in shallow mixing case profile 80 float 6901493 MLD=34.5m, ipar_15=79.4m

deep mixing cases (MLD > ipar_15) without considering the light threshold

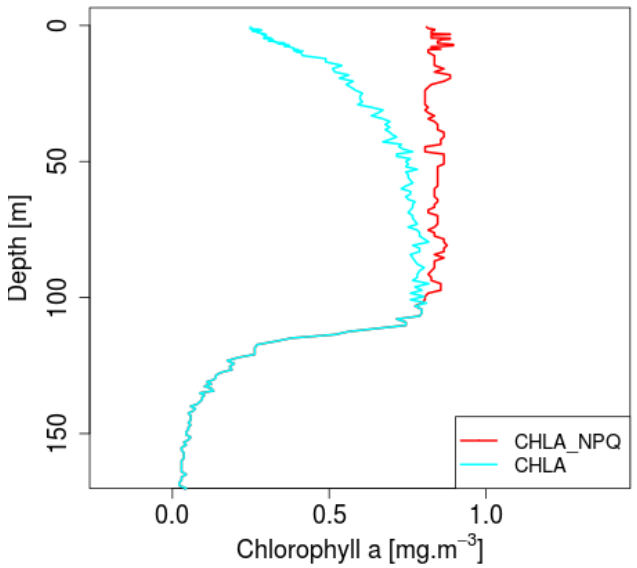

Figure 7 : Example of NPQ correction in deep mixing case profile 40, float 6901493 MLD=113.6m, but without the light threshold limit (ipar_15=60.2m), so the maximum of the CHLA/BBP is estimated within the whole mixed layer.

We can see that ignoring the light threshold limit (Figure 7) leads to a slightly bigger estimation of the NPQ corrected CHLA than on Figure 5.

shallow mixing cases (MLD < ipar_15) without considering the light threshold

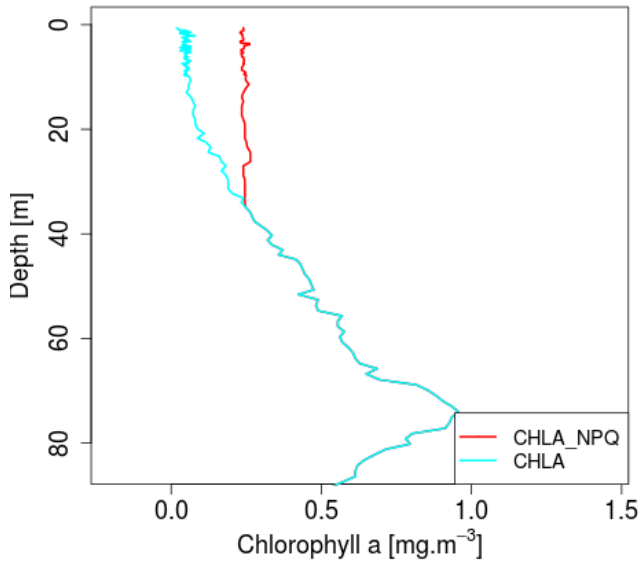

Figure 8: Example of NPQ correction in shallow mixing case profile 80 float 6901493 MLD=34.5m but without the light threshold limit (ipar_15=79.4m), so the maximum of the CHLA/BBP is estimated within the whole mixed layer, while the light penetrates deeper than the MLD.

We can see that accounting for the light threshold limit (Figure 6) leads to a bigger estimation of the NPQ corrected CHLA (+0.2mg.m-3) than on Figure 8.

In conclusion, the "Terrats" method is proposed to estimate the NPQ correction in the delayed mode quality control of CHLA. Light information is an asset mainly for shallow mixing profiles.

3.2.2 SLOPE CORRECTION

3.2.2.1 General introduction on the main philosophy

The SLOPE factor is the value which is used to transform fluorescence in chlorophyll a and it is generally factory calibrated. In RT, a fixed value (egal to 2, is used: The value used in RT is obtained from the results of Roesler et al. (2017), who demonstrated that the SLOPE factor is regionally variable (see Figure 9), ranging from 1 to 6, with a median value around 2. This value (2 or its inverse 1/2) is to be linked with the last equation of Figure 3, the Roesler adjustment :

CHLA_ADJUSTED=CHLA_ADJUSTED/2

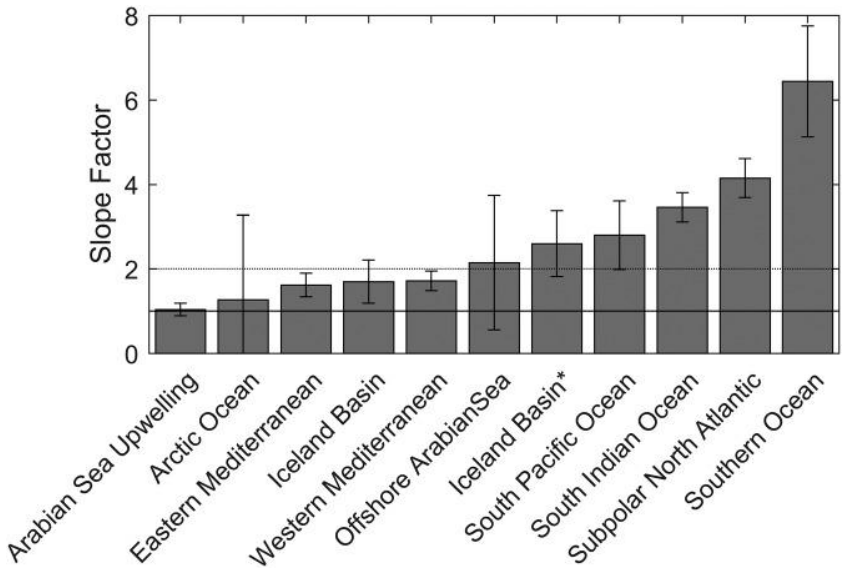

Figure 9: Slope factors estimated with HPLC comparisons in different basins.

As a part of the DMQC, it is mandatory to caracterise, and possibly correct, the spatial (and probably also temporal) variability of the SLOPE factor.

The critical point to solve the issue is that systematic (and concomitant with floats profiles) chlorophyll observations are scarce, and it is virtually impossible to verify the SLOPE factor variability at global scale. Alternative evaluations of chlorophyll could however be used to check the chlorophyll-to-fluorescence ratio. A very promising approach implies the radiometric inversion of irradiance floats profiles (Xing et al. 2011), which could provide an estimation of chlorophyll which is independent to fluorimetric data. Moreover, recent neural network methods (i.e. SOCA, see later) provide estimations of SLOPE factor by combining fluorescence float profiles with surface (i.e. satellite) data. This assessment of SLOPE factor could provide an alternative validation of the SLOPE estimation and it will be used to validate (with the available HPLC data) the approach. In the following sections we will refer to the slope factor as the inverse of the SLOPE factor presented in Figure 9, as the last multiplicative factor that should be applied to CHLA_ADJUSTED.

3.2.2.2 Implementation

3.2.2.2.1 Floats equipped with radiometer

Most of the European floats equipped with fluorometers are also equipped with radiometers, so this slope can be determined following Xing et al., (2011) method, using Ed490 profiles. For floats equipped with radiometers, we will test the stability of the Xing et al., 2011, at the float

scale estimating the slope for every profile to check that the value is quite stable over the whole float life. Then, we have seen (Figure 9) that this slope is regionally changing, so in order to check its stability at a basin scale, we have estimated the slopes for every profile of every float in the same area and calculate theirs median per month to check the stability of the value through the months of the year.

3.2.2.2.2 Floats not equipped with radiometer

For floats not equipped with radiometers, we calculated Ed490 profiles using the method SOCA-Radiometry. In Sauzède et al. (2016), the authors developed a machine learning-based method that efficiently extends surface bio-optical properties (i.e. particulate backscattering) to depth. This method, so-called SOCA for "Satellite Ocean Color merged with Argo data", relies on the merging of ocean color observations with in situ hydrological properties to infer the vertical distribution of bio-optical properties. SOCA is trained using BGC-Argo hydrological and bio-optical profiles matched with satellite data. It has been recently upgraded to retrieve other bio-optical properties measured from BGC-Argo floats such as the CHLA (SOCA-CHL) or the SOCA-Radiometry (PAR or Ed490). The SOCA-Radiometry method uses the PAR or the irradiance fields for the training. Once the trained optimised, SOCA provides Ed490 profiles using as input data satellite (Globcolour) matchups (PAR, reflectances at different wavelengths), temperature and salinity profiles of the float. These Ed490 synthetic profiles are then used following Xing et al. 2011, to determine the SLOPE.

We will first compare for a float (6901472) equipped with a radiometer and not in the training set, Ed490 and synthetic Ed490 profiles. Then for 5 floats in different areas, without radiometers, we will use Ed490 synthetic profiles to determine the SLOPE and apply it at the third step of the DM procedure and compare the DM fields with ocean color data.

3.2.2.3 Results for floats equipped with radiometer

3.2.2.3.1 Stability of the SLOPE at the float scale

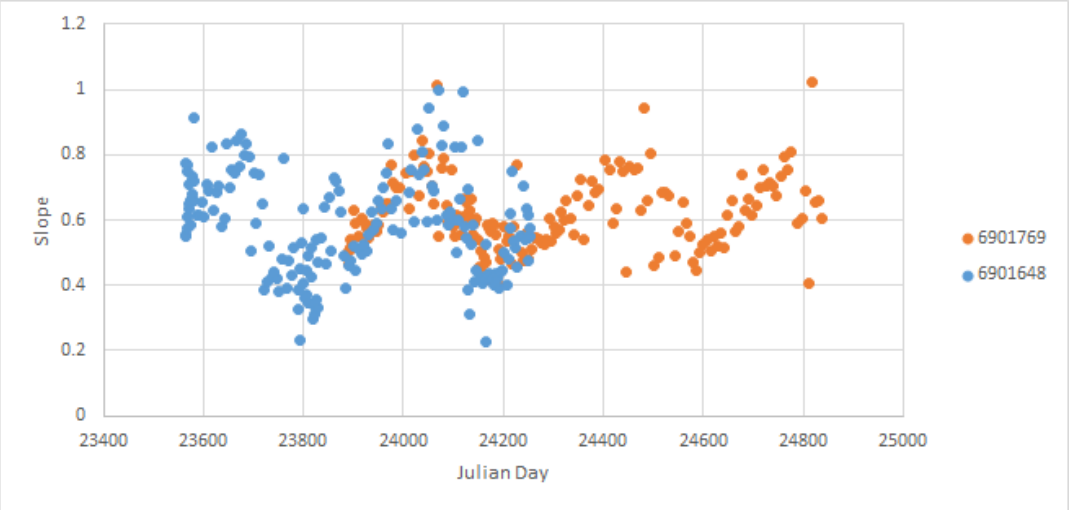

Figure 10 : Variation of the Xing et al., 2011 slope estimation through time for two floats deployed in the Mediterranean western Basin (6901648 and 6901769)

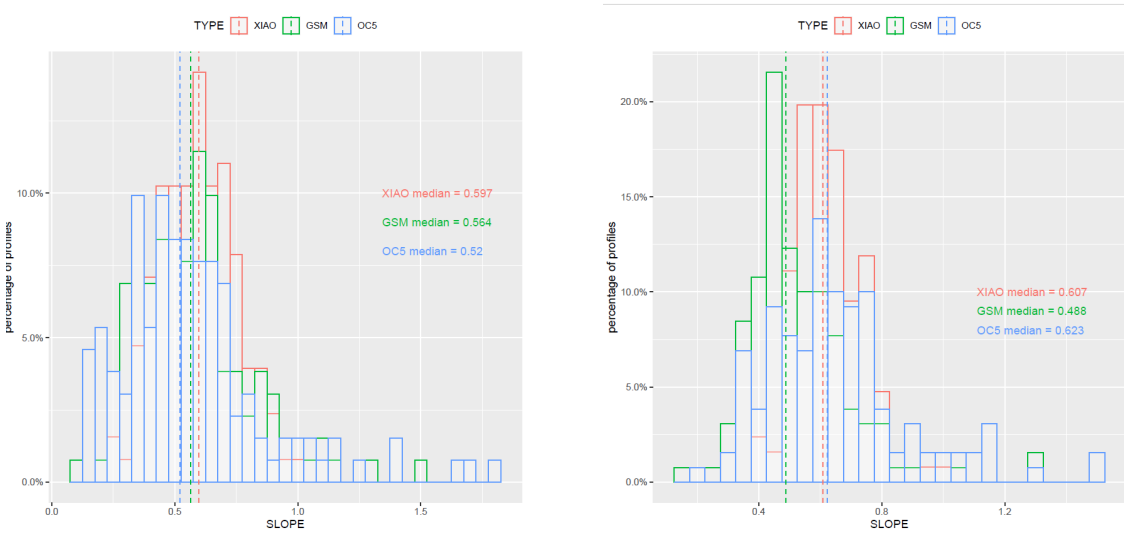

Figures 11 : 6901648 and 6901769 histograms of slope estimation based on Xing et al., 2011 and by comparison with Ocean colour data (GSM and OC5 algorithms)

3.2.2.3.2 Stability of the SLOPE at the basin scale

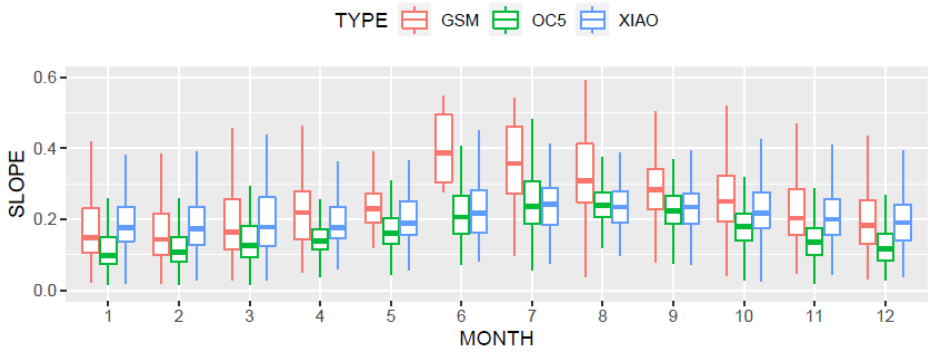

Figure 12a : Southern Ocean basin: seasonality of the slope retrieved by Xing et al., 2011 and with OC5 and GSM products

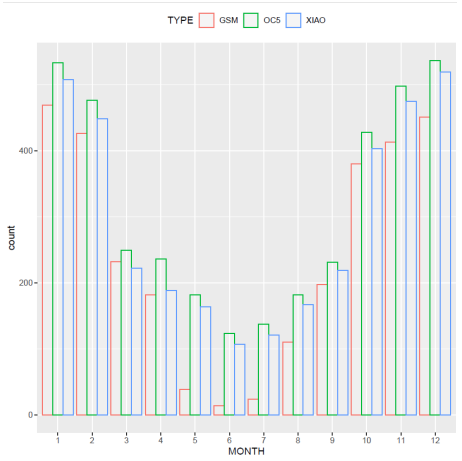

Figure 12b : Southern Ocean basin : number of profiles available to estimate the slope at the basin scale

We can see on Figure 12b, that there are fewer available GSM data particularly in June, July and August (Southern hemisphere winter). As a consequence the slope estimated with Xing et al., 2011, as well as OC5 data do not compare very well during these months (Figure 12a).

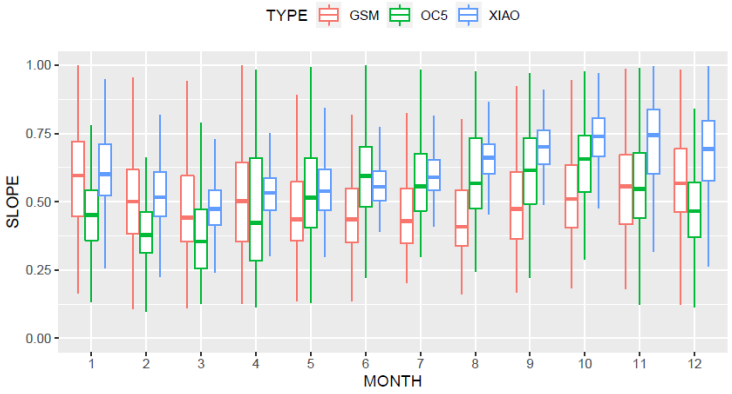

Figure 13a : North western Mediterranean basin: seasonality of the slope retrieved by Xing et al., 2011 and with OC5 and GSM products

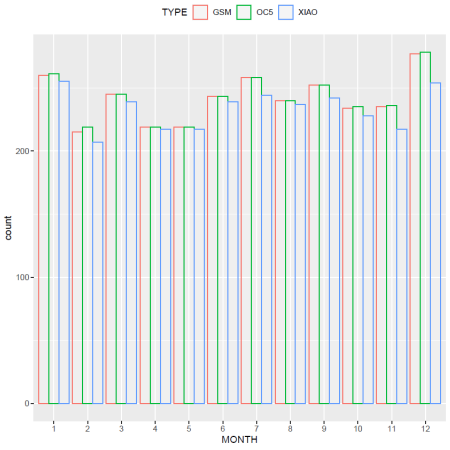

Figure 13b : North western mediterranean basin : number of profiles available to estimate the slope at the basin scale.

Compared to the Southern Ocean basin (Figure 12b), we can see for the Western Mediterranean Basin that the number of profiles available for each month is very stable through the year (Figure 13b), it will then allow in the future to estimate a relevant seasonal trend. We can see a seasonality of the slope in Figure 13b, like the one we saw on Figure 10. This seasonality is not in the same order of magnitude than the slope itself, so as a first guest, we choose to ignore this seasonality trend and focus on the median of the slope (the seasonality of the slope will be investigated in the coming months, mainly for well sampled basin like the Mediterranean sea). For other areas, like in the Southern ocean in May, June, July and August, there are less available profiles for the comparison and building a seasonality could be more tricky. Maps of slopes estimated for floats equipped with radiometer are in Annexes 6.2.1

In conclusion, for floats equipped with radiometers, we suggest as a first guess to use the median of the SLOPE retrieved with Xing et al., 2011. The seasonality of the SLOPE needs to be further investigated considering the limitations of the light in winter and the need to have a very well sampled basin.

3.2.2.4 Results for floats not equipped with radiometer

In the previous section, we highlight how the profile of irradiance Ed490 measured by radiometers in combination with the fluorescence can be used to estimate the slope. Now, we will focus on results for floats not equipped with radiometers. As a preliminary result, we compare for a float (6901472) equipped with a radiometer and not in the SOCA-Radiometry training set, Ed490 and synthetic Ed490 profiles.

3.2.2.4.1 Validation of the synthetic Ed490 profiles

First, we compare for a float (6901472) equipped with a radiometer and not in the training set , Ed490 and synthetic Ed490 profiles.

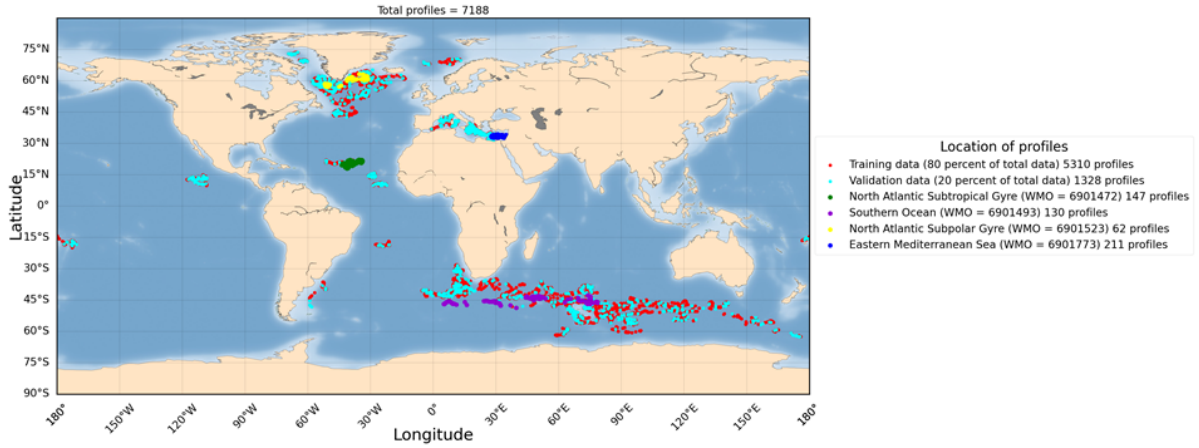

Figure 14: (Courtesy of Renosh Pannimpullath) Ed490 profiles used to train and validate the SOCA method developed to retrieve the vertical distribution of Ed490 from merged Argo and ocean color data

Float 6901472 is equipped with a radiometer and is part of the independent validation dataset for the neural network (these time series were initially removed from the training and validation datasets composed of 80% and 20% respectively of the data). First, we present here a comparison of the Ed490 from float and Ed490 computed from SOCA using Globcolour satellite matchups as inputs on Figure 15. On the left panel, there is a comparison of the two profiles (real and synthetic) and on the right panel, the same profile as a scatter plot . We can see on Figure 15, how the synthetic profile is comparable to the real profile.

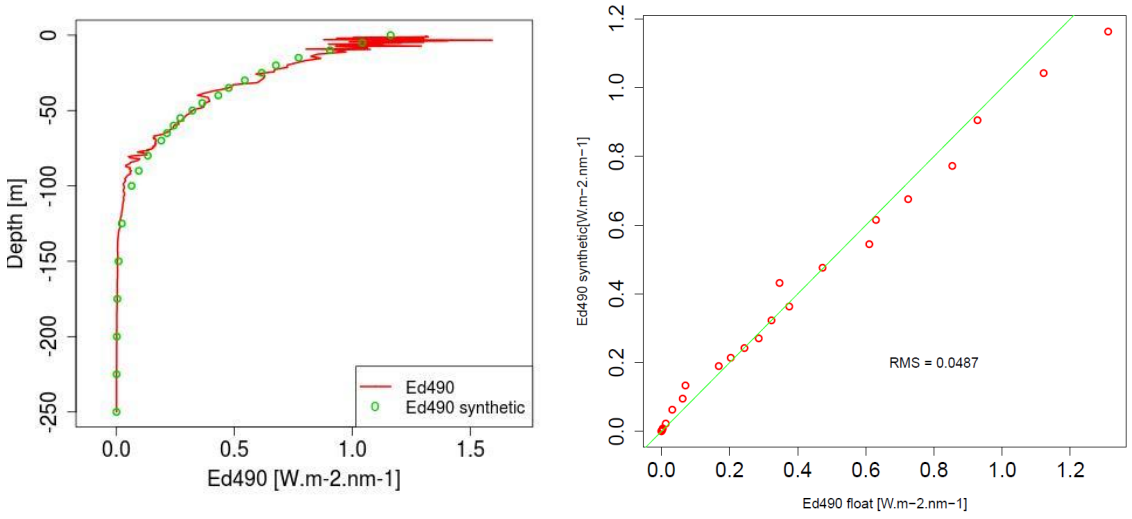

Figure 15 : Comparison of Ed490 profile from float data and as computed from SOCA-Radiometry using Globcolour satellite matchups as inputs for **float 6901472**, profile 3 and its associated scatter plot.

Once we have highlighted that the SOCA-Radiometry allows to retrieve satisfactorily synthetic Ed490. For all profiles with satellite matchups, we compute a synthetic profile of Ed490, then we use the Xing et al., 2011 method to retrieve the slope (SLOPE_SYNTHETIC) with CHLA profiles corrected of the dark value and the quenching. Then we compare the SLOPE_SYNTHETIC to the SLOPE, to check their coherence.

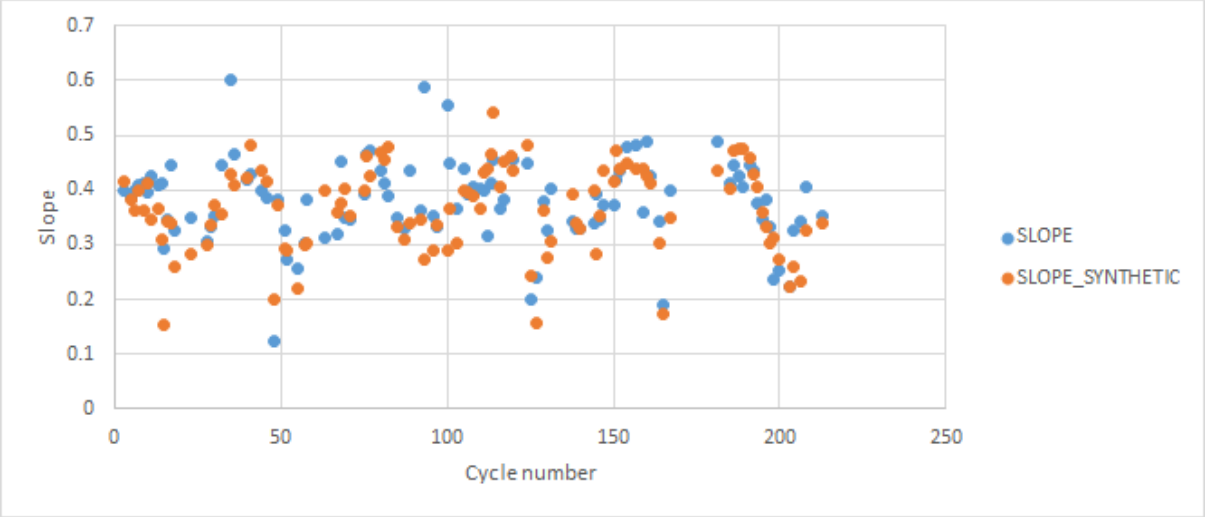

Figure 16 : Variation of the Xing et al., 2011 slope estimation through cycles for float 6901472 with Ed490 float data and synthetic profiles of Ed490, computed from SOCA-Radiometry

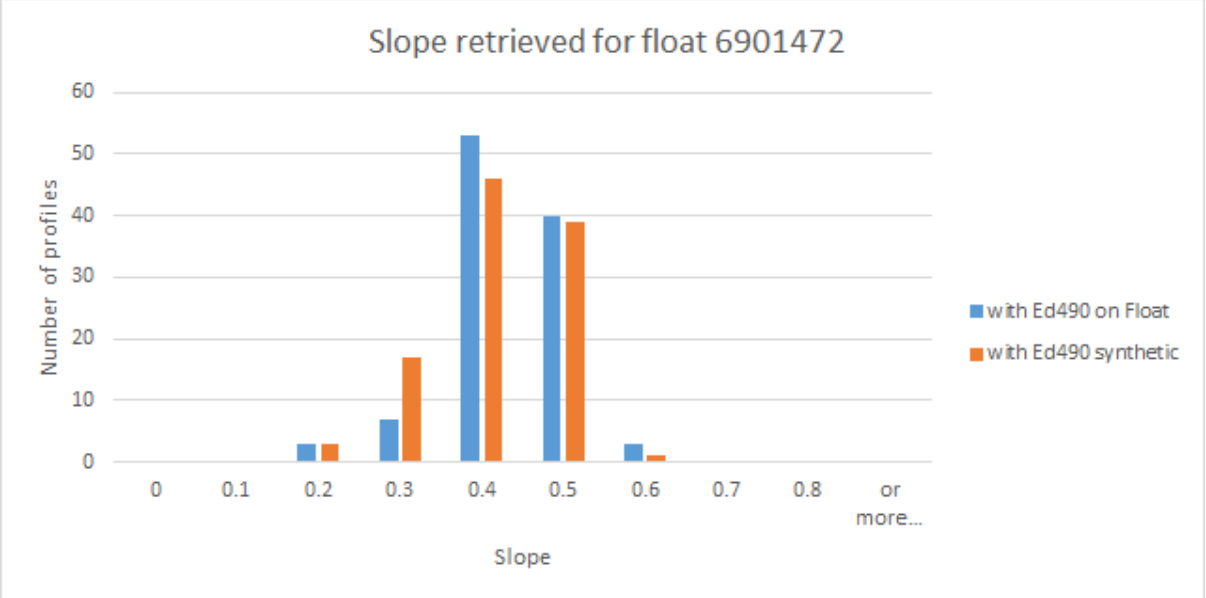

Figure 17 : Histogram of the Xing et al., 2011 slope estimation for float 6901472 with Ed490 float data and synthetic profiles of Ed490, computed from SOCA-Radiometry

	MEDIAN SLOPE	SD
With Ed490 Argo (all)	0.387	0.073
With Ed490 synthetic (all)	0.371	0.078
With Ed490 Argo (both)	0.387	0.075
With Ed490 Synthetic (both)	0.366	0.078

Table 1 : Comparison of the median and STD of the Xing et al., 2011 slope estimation for 6901472 with Ed490 float data and synthetic profiles of Ed490, computed from SOCA-Radiometry.

We can see on Table 1 that the median slope retrieved with real profiles of Ed490 compared to values retrieved with synthetic profiles during the whole float life with real profiles are very close.
Maps of slopes estimated for floats not equipped with radiometer are in Annexes 6.2.2

In conclusion, for floats not equipped with radiometers, we suggest to use the SOCA-Radiometry method to compute synthetic Ed490 and use them with Xing et al., 2011 method to retrieve the SLOPE.

3.2.2.4.2 Testing the DM procedure performed with a SLOPE estimated from synthetic Ed490 profiles

For 5 floats in different areas, without radiometers, we will use Ed490 synthetic profiles to determine the SLOPE and apply it as the third step of the DM procedure and compare the DM fields with ocean color data (GSM and OC5).

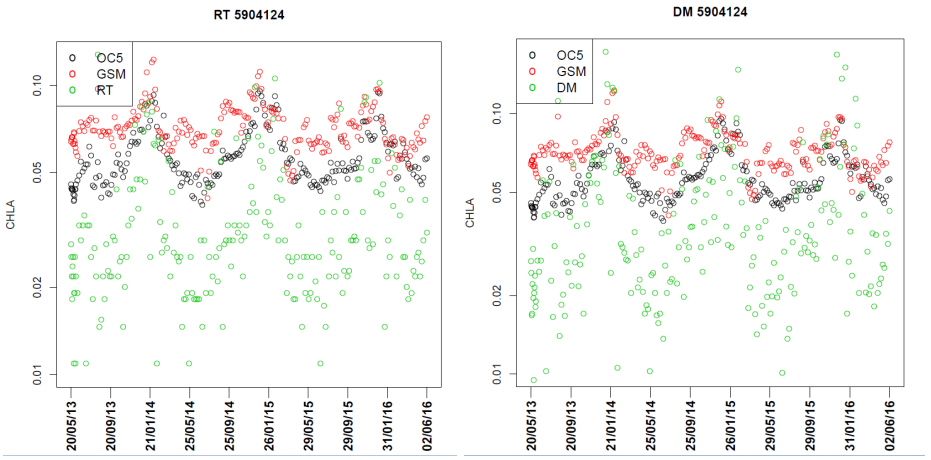

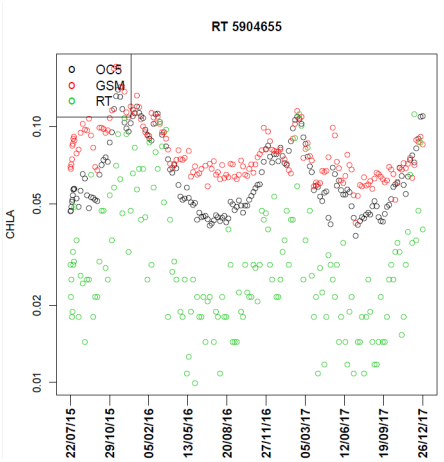
RT 5904655
OC5
GSM
RT
CHLA
0.01
0.02
0.05
0.10
22/07/15
29/10/15
05/02/16
13/05/16
20/08/16
27/11/16
05/03/17
12/06/17
19/09/17
26/12/17

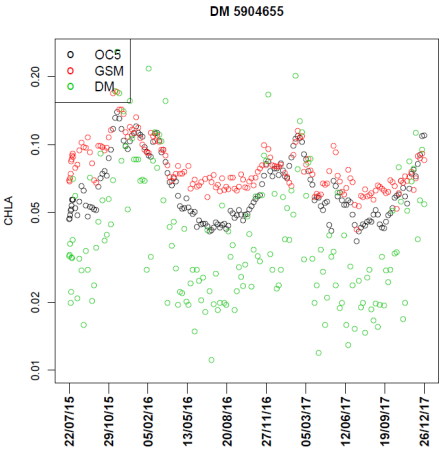
DM 5904655
OC5
GSM
DM
CHLA
0.01
0.02
0.05
0.10
0.20
22/07/15
29/10/15
05/02/16
13/05/16
20/08/16
27/11/16
05/03/17
12/06/17
19/09/17
26/12/17

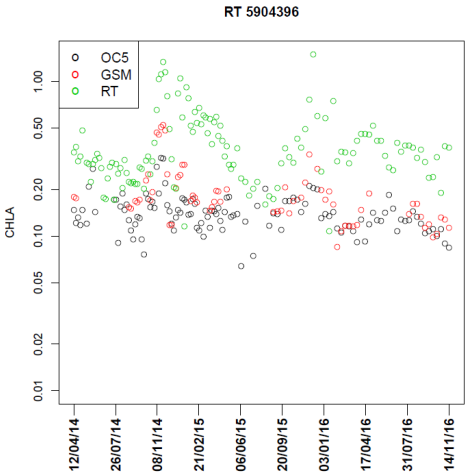
RT 5904396
OC5
GSM
RT
CHLA
0.01
0.02
0.05
0.10
0.20
0.50
1.00
12/04/14
26/07/14
08/11/14
21/02/15
06/06/15
20/09/15
03/01/16
17/04/16
31/07/16
14/11/16

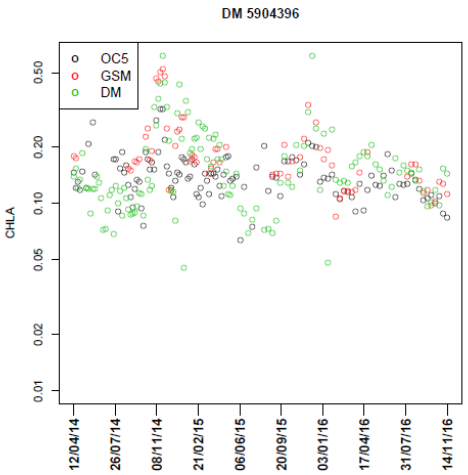
DM 5904396
OC5
GSM
DM
CHLA
0.01
0.02
0.05
0.10
0.20
0.50
12/04/14
26/07/14
08/11/14
21/02/15
06/06/15
20/09/15
03/01/16
17/04/16
31/07/16
14/11/16

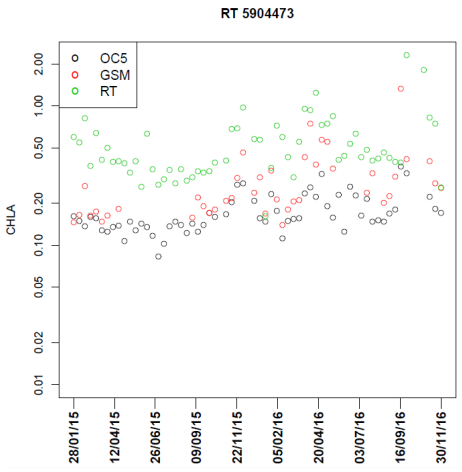
RT 5904473
OC5
GSM
RT
CHLA
0.01
0.02
0.05
0.10
0.20
0.50
1.00
2.00
28/01/15
12/04/15
26/06/15
09/09/15
22/11/15
05/02/16
20/04/16
03/07/16
16/09/16
30/11/16

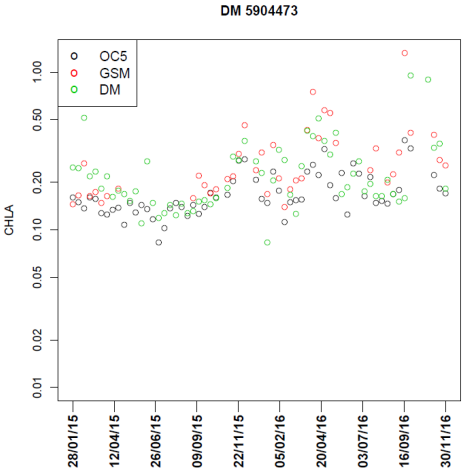
DM 5904473
OC5
GSM
DM
CHLA
0.01
0.02
0.05
0.10
0.20
0.50
1.00
28/01/15
12/04/15
26/06/15
09/09/15
22/11/15
05/02/16
20/04/16
03/07/16
16/09/16
30/11/16

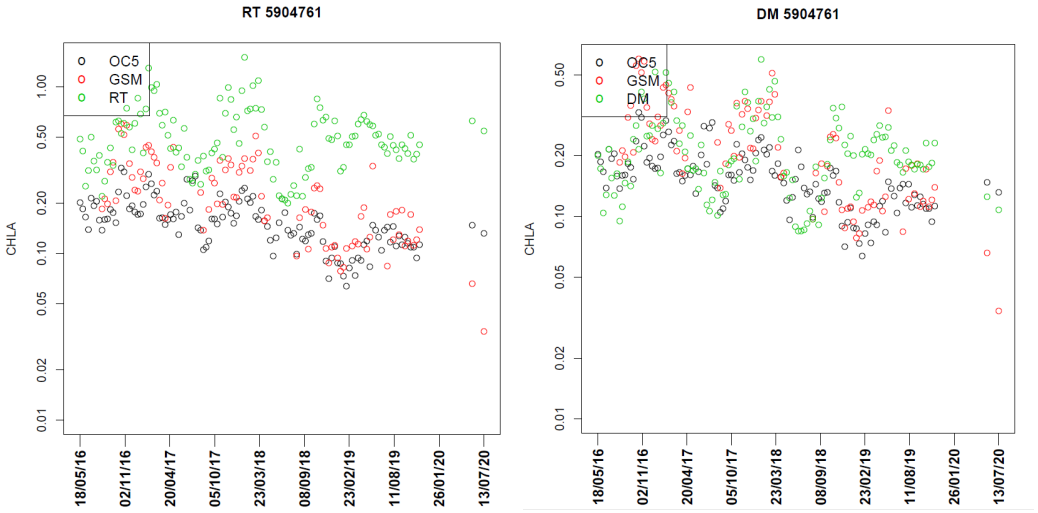

Figure 18 : Results of DM procedures applications (Left panels PARAMETER_DATA_MODE="A", Right panels PARAMETER_DATA_MODE="D") on 5 floats not equipped with radiometers.

WMO	MODE	RMSE_GSM	RMSE_OC5
5904124 (NP)	A	0.0418	0.028
5904124 (NP)	D	0.0396	0.028
5904655 (NP)	A	0.0510	0.0368
5904655 (NP)	D	0.0447	0.0339
5904396 (SP east)	A	0.3175	0.3552
5904396 (SP east)	D	0.0701	0.0899
5904473 (SO)	A	0.4692	0.4598
5904473 (SO)	D	0.2272	0.1282
5904761 (SP West)	A	0.3965	0.4180
5904761 (SP West)	D	0.1089	0.1117

Table 2 : comparison of RMS for PARAMETER_DATA_MODE= A or D, calculated over the whole float life between CHLA_ADJUSTED and OC data (GSM, OC5) for aoml floats with slope estimated with synthetic Ed490 profiles. (NP= North Pacific, SP=South Pacific, SO=Southern Ocean)

For the 5 floats results displayed, we can see on Figure 18 while comparing the left panels (PARAMETER_DATA_MODE="A") to the right panels (PARAMETER_DATA_MODE="D") that visually applying the DM procedures reduces the dispersion of the floats data compare to both satellite products. This visual impression is all the more important with high values of CHLA concentrations (5904396, 5904473, 5904761) compare to low CHLA concentrations (5904124, 5904655). Table 2 shows that in every case (low or high concentrations), applying the DM procedures reduces the RMS between the BGC-Argo and both satellite products (OC5 or GSM).

3.2.3 SUMMARY of the different steps

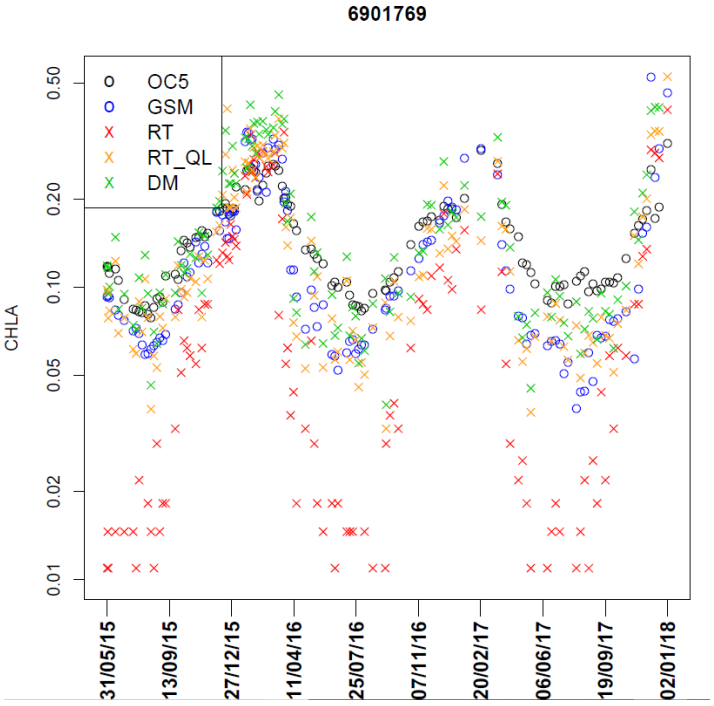

Figure 19: Illustration of the main steps of the Delayed mode procedures. Red Crosses : CHLA_ADJUSTED , PARAMETER_DATA_MODE="A" , NPQ (Xing et al 2012), Orange crosses : CHLA_ADJUSTED = 0.5 *CHLA_ADJUSTED, NPQ (Terrats et al., 2020), Green crosses : CHLA_ADJUSTED, PARAMETER_DATA_MODE="D". Black and blue circles: respectively OC5 and GSM satellite products.

Figure 19 illustrates the whole application of the DM procedures and particularly highlights the effect of changing the method to estimate the quenching correction, mainly on low CHLA concentrations. When we compare red crosses to orange crosses, the differences are noticeable (the effect is emphasized by the use of logarithmic scale). The slope correction is less impressive here as the floats is in the Mediterranean sea (with slope estimation by Xing 2011 0.609, close to the Roesler Factor of 0.5)

3.3 Delayed Mode Quality Control operational

This part is dedicated to help DM operators to perform their DM by providing tools and ways to evaluate their correction.

3.3.1 Visual control

The preliminary step of the DMQC is to set a QC=4 for profiles and levels that obviously reported an issue and then to prevent them from being considered in the estimation of the adjustment.

SCOOP-Argo (https://doi.org/10.17882/48531) is a tool developed at Coriolis for visual inspection of Argo profiles (Detoc et al., 2021) that allows to plot every station one by one or among the other profiles. This last option allows us to see quite rapidly which profiles are outliers.

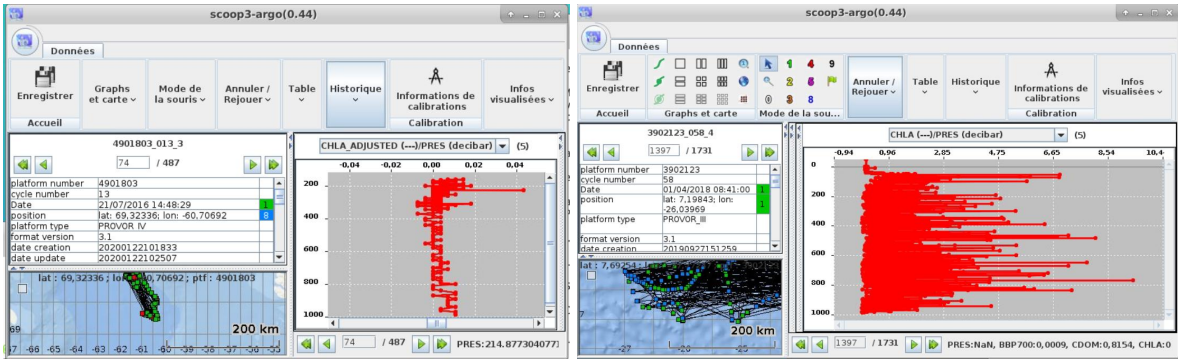

Figure 20 : On the left, visual inspection for the float 4901803, (very low values of CHLA => QC=4). On the right, visual inspection for the float 3902123 (numerous spikes => QC=4)

This step allows to remove levels or entire profiles that are obviously bad in the next steps of the delayed mode procedure.

3.3.2 Estimation of the correction

3.3.2.1 Dark correction

Resulting from the aforementioned R & D work on dark offsets, a tool was developed to be used in the production of CHLA delayed mode (https://github.com/qjutard/dark_offset_chla). For a given float, this tool plots the median filtered minima of the profiles and the median of all minima, which is the method considered in the R&D work. From this, and from CHLA time series that can be visualized with another tool we provide (https://github.com/qjutard/time_series_plot), a DM operator can validate that the median adequately represents the minima distribution. If the median is not a satisfying value there is the possibility to replace it with a running median, this can mainly be used to account for sensor drift.

An example of outputs from these tools is given on Figure 21 for float 6901439. These float started outputting bad data around profile 270, the bar on top of the DARK visual tells the operator that it was indeed put on the greylist. This bar is color coded from green to red to indicate the percentage of bad data in each profile, and is grey or black for profiles on the greylist, here the data is flagged as very good (full green) up until the float is put on the greylist. The operator then notes that the sensor seems to drift towards lower values, especially around the end of the non-greylist series. They can confirm that this drift exists from the BGTS visual, noting that all this trend in the minima is representative of a trend in all the water column. From this, the operator decides that the median of minima is not satisfying for this float and runs a

running median on the same minima, here they choose a default filter size of 51. From there the operator can decide whether the offsets are satisfying or not, in the latter case they can increase or decrease the size of the filter. In Figure 21 we see that the filter doesn't quite reach the highest minima at the beginning of the series, or the lowest minima at the end, but given the 1-2 counts noise we observe the filter size of 51 can be considered adequate.

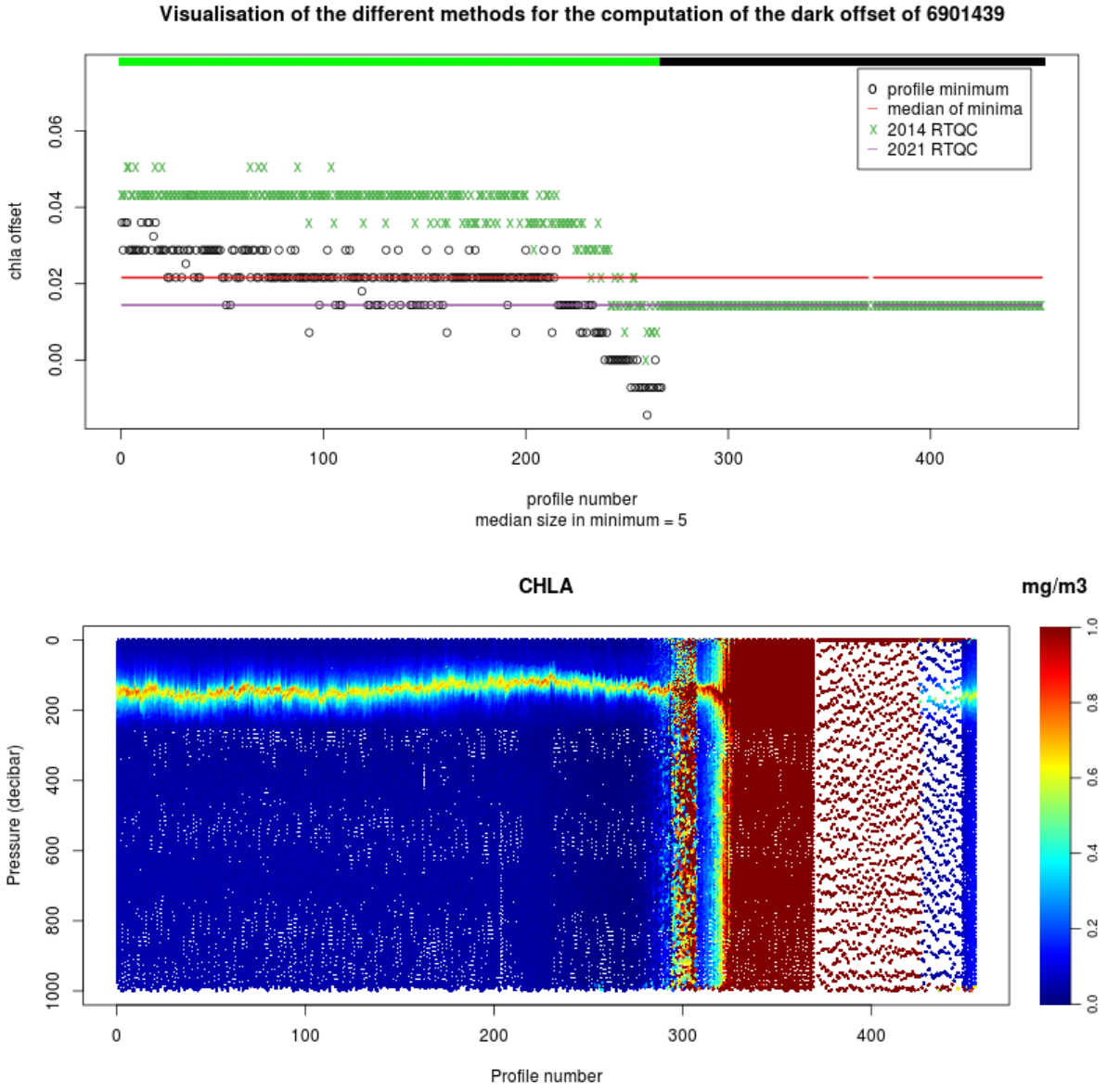

Figure 21 : Example of combination of the Dark (on top) and BGTS (Time series) tools that can be used by a DM operator to select DARK offset values for Float 6901439

Once the DM operator has obtained satisfying values for the dark offset, this value is an input of the following NPQ correction.

3.3.2.2 Non photochemical Quenching Correction

As stated in the R&D section, the correction for NPQ has been tested and adapted to be used on the whole data fleet. It is based on the ratio between BBP and CHLA and introduces a light threshold criteria, to

We distinguish 3 types of floats:

1. Floats with fluorometer, radiometer and BBP sensors
2. Floats with Fluorometer and BBP sensors
3. Floats with Fluorometers

A tool has been developed to apply a quenching correction on floats of type 1 and 2, https://github.com/catsch/STEP2_QUENCHING (to be completed with Xing et al., 2012 option) , this tool also assigns QC=5 for levels in the quenching area.

Applying this Non Photochemical Quenching correction implies that there is a correlation between CHLA and BBP. This correlation might fail, for example in case of strong dust events or in case of BBP sensor issue, so before moving to the STEP3 (slope estimation), it is recommended to perform a quick visual QC test to check that the NPQ correction doesn't create spikes, linked to dust seen by the BBP sensor and not related to CHLA and to prevent eventual outliers to enter the slope estimation.

3.3.2.3 Slope Correction (Courtesy X. Xing, P. Renosh)

<u>For floats equipped with radiometers</u>

Xing et al. (2011) has developed a tool to estimate operationally the slope using both the Ed490 profile and the CHLA profile corrected of the Dark and of the Non Photochemical Quenching (STEP1 and STEP2). This tool will soon be available, here : https://github.com/catsch/STEP3_SLOPE and presently can be used on request.

<u>For floats without radiometers</u>

A tool has been developed to estimate a synthetic profile of Ed490 using both T/S profiles and satellite matchups. This synthetic profile Ed490 profiles associated with the CHLA profile corrected of the Dark and of the Non Photochemical Quenching (STEP1 and STEP2) are then used as inputs for the former Xing et al. (2011) tool, to estimate operationally the slope. This tool will soon be available, here : https://github.com/catsch/STEP3_SLOPE and presently can be used on request.

3.3.3 Evaluation of the correction

3.3.3.1 Comparison with HPLC data

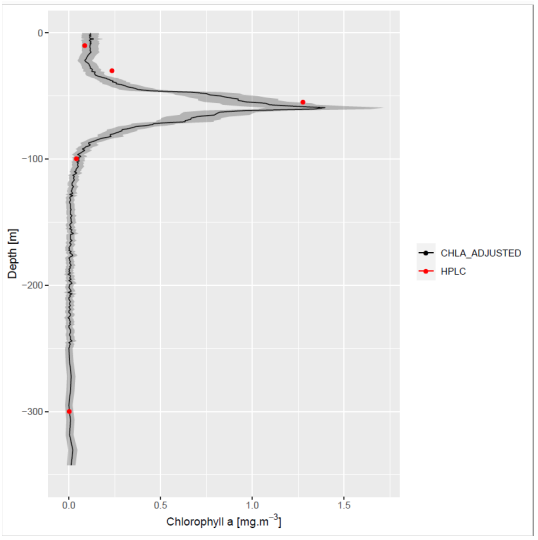

Figure 22 : Comparison of CHLA_ADJUSTED in DM (DARK, NPQ, SLOPE) with HPLC measurements at deployment for float 6901653

On Figure 22, we present the "promising" results of the comparison between a profile in DM and the synchronous (in space and time) HPLC (Collection and High Pressure Liquid Chromatography) measurements. HPLC analysis of discrete water samples adjacent to and synchronous with fluorometer observations is the community-accepted validation product (Roesler et al., 2017) of the BGC-Argo CHLA parameter. Anyway for more than 100 floats with fluorometers in the Coriolis DAC, we only have those matchups for a third of them. They were mainly acquired at the deployment of the floats.

3.3.3.2 Comparison with Satellite data

To evaluate the correction our results are compared with satellite data.

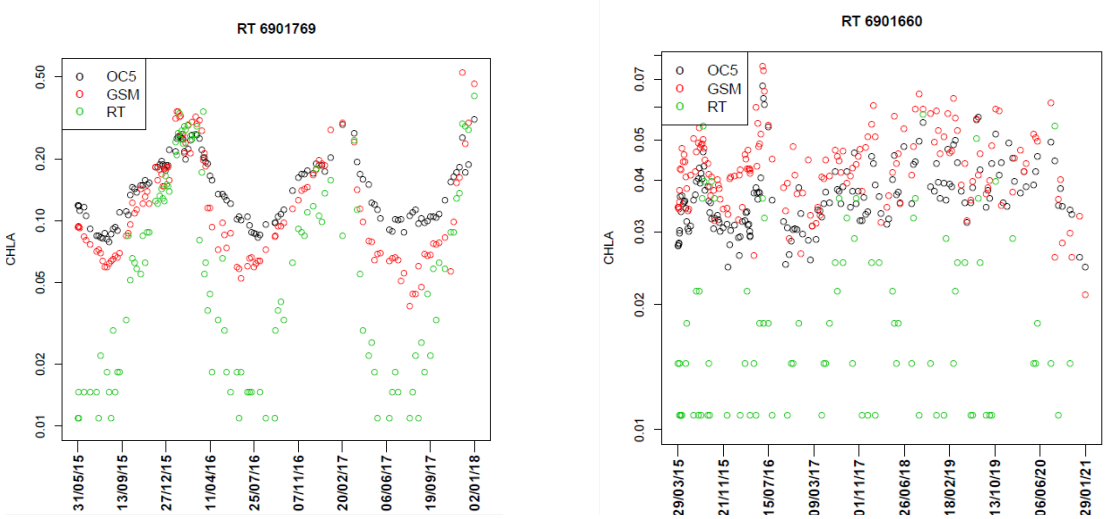

Figure 23: comparison of the adjustment in RT (PARAMETER_DATA_MODE="A") (green circles) to two satellite CHLA products retrieved by two algorithms (GSM : Red circles, OC5 : black circles) during the whole life of two floats : 6901769 in the Mediterranean sea, 6901660 in the Pacific Ocean.

We can see on Figure 23 that the main issue regarding the Real Time adjustment is related to very low concentrations of CHLA. The float 6901769 explores a wide range of CHLA values from 0.01 to 0.5 and we can see that the major discrepancies between float data and satellite data occur for concentrations from 0.01 to 0.05, this visual impression is for sure emphasized by the use of logarithmic scale. There can be two explanations, the CHLA concentrations are not proportionally accurately retrieved by satellites and the RT non photochemical quenching correction underestimates the CHLA concentrations.

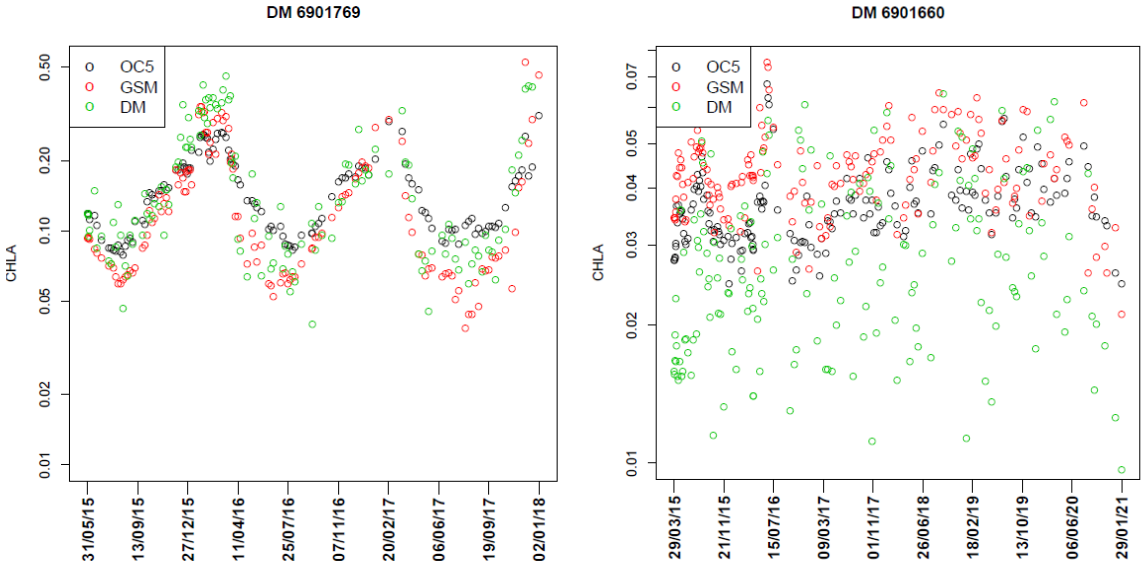

Figure 24 : comparison of the adjustment in DM (PARAMETER_DATA_MODE="D") (green circles) to two satellite CHLA products retrieved by two algorithms (GSM : Red circles, OC5 : black circles) during the whole life of two floats : 6901769 in the Mediterranean sea, 6901660 in the Pacific Ocean.

WMO	MODE	RMSE_GSM	RMSE_OC5
6901769	A	0.0662	0.0826
6901769	D	0.0586	0.0655
6901660	A	0.0330	0.0259
6901660	D	0.0194	0.0139

Table 3 : comparison of RMS for PARAMETER_DATA_MODE= A or D, calculated over the whole float life between CHLA_ADJUSTED and OC data (GSM, OC5)

We can see on Figure 24, compared to Figure 23, that visually applying the DM procedures reduces the dispersion of the floats data compared to both satellite products. Once again, this visual impression is all the more important with higher values of CHLA concentrations (6901769) compare to low CHLA concentrations (6901660). Table 3 shows that in every case (low or high concentrations), applying the DM procedures reduces the RMS between the BGC-Argo and both satellite products (OC5 or GSM).

3.3.3.3 Comparison with SOCA-CHL (Perspectives)

The SOCA (for Satellite Ocean Color merged with Argo data to infer bio-optical properties to depth, Sauzède et al. 2016) developed for the retrieval of the vertical distribution of Chl is trained using the BGC-Argo CHLA_ADJUSTED data of reference. This SOCA method is validated using a totally independent global database of ~1600 profiles of Chl determined by HPLC. Using this validation database, several SOCA-Chl models can be evaluated by changing the CHLA_ADJUSTED data used for the training. Theoretically, the more accurate the CHLA_ADJUSTED will be, the better will be the validation of SOCA-Chl estimates against HPLC reference data. Thus, using this methodology it becomes possible to globally validate the impact of Chl delayed mode data processing.

3.3.4 Fill the DM information and error estimation

After every steps of the correction :

- STEP 1 : Dark correction
- STEP 2 : NPQ correction
- STEP 3 : Slope correction

The DM filler tool (https://github.com/catsch/DM_FILLER) can be used to enter the correction and provide BD files with PARAMETER_DATA_MODE=”D” for CHLA.

here are the recommendations for example for Floats equipped with Radiometers and BBP sensors :

SCIENTIFIC_CALIB_EQUATION : “CHLA_ADJUSTED =(CHLA - OFFSET) * SLOPE”

For Float 6901769 :

SCIENTIFIC_CALIB_COMMENT : “Slope, Xing et al. 2011- Quenching, Xing et al., 2018, Terrats et al., 2020”

SCIENTIFIC_CALIB_COEFFICIENT : “OFFSET= 0.0365 , SLOPE= 0.604”

For float with radiometers and BBP sensors, like 6901769:

CHLA_ADJUSTED_ERROR = Max [0.02 ; SD/slope * CHLA_ADJUSTED]

For float without radiometers and BBP sensors :

CHLA_ADJUSTED_ERROR = Max [0.05 ; SD/slope * CHLA_ADJUSTED]

4 Conclusions and perspectives

We synthesised on the following scheme (Figure 25) what would be the different steps of the procedures to perform DM on the CHLA parameter followed by a float according to the different companions sensors on board.

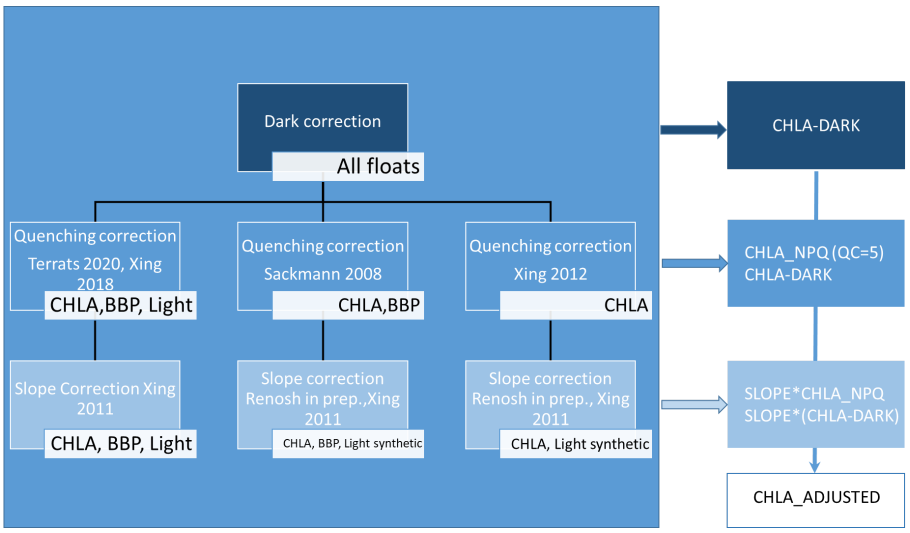

Figure 25: Summary of different ways to perform DM depending on different sensors on board.

Different methods were presented in this deliverable to be able to estimate the calibration factors (DARK and SLOPE) and to correct for the Non Photochemical Quenching for all different sensor configurations on board. These methods were widely tested on more than 300 floats, results are presented both in the core documents and in the Annexes (results presented in the Annexes need a stringent visual control before being considered as delayed mode results). In the coming months,

these methods will be used at the global scale (presently, only floats in the Mediterranean Sea were corrected). Once published, SOCA-Radiometry, that allows to infer radiometric information, will be publically available. Results are already available on request. Finally, the method SOCA-Chl offers a way to assess the accuracy of the DM procedure at the global scale and its application is foreseen once a large number of floats has been corrected in DM.

5 References

Marco Bellacicco, M. Cornec, E. Organelli, R. Brewin, G. Neukermans, et al.. Global variability of optical backscattering by non-algal particles from a Biogeochemical-Argo dataset. Geophysical Research Letters, American Geophysical Union, 2019, 46 (16), pp.9767-9776. https://doi.org/10.1029/2019GL084078

Detoc Jerome, Garo Mickael, Carval Thierry, Thepault Baptiste, Mahoudo Pierre (2017). Scoop-Argo : visual quality control for Argo NetCDF data files. SEANOE. https://doi.org/10.17882/4853.

Lavigne, H., F. D'Ortenzio, H. Claustre, and A. Poteau (2012). Towards a merged satellite and in situ fluorescence ocean chlorophyll product. Biogeosciences 9, 2111–2125, https://doi.org/10.5194/bg-9-2111-2012

Roesler C, Uitz J, Claustre H, Boss E, Xing X, Organelli E, Briggs N, Bricaud A, Schmechtig C, Poteau A, D'Ortenzio F, Ras J, Drapeau S, Haentjens N, Barbieux M (2017) Recommendations for obtaining unbiased chlorophyll estimates from in situ chlorophyll fluorometers: a global analysis of WET Labs ECO sensors. Limnol Oceanogr-meth | https://doi.org/10.1002/lom3.10185.

Sackmann, B. S., Perry, M. J., and Eriksen, C. C.: Seaglider observations of variability in daytime fluorescence quenching of chlorophyll-a in Northeastern Pacific coastal waters, Biogeosciences Discuss., 5, 2839–2865, https://doi.org/10.5194/bgd-5-2839-2008, 2008.

Sauzede, R., Claustre, H., Jamet, C., Uitz, J., Ras, J., Mignot, A. and F. D'Ortenzio (2015). Retrieving the vertical distribution of chlorophyll a concentration and phytoplankton community composition from in situ fluorescence profiles: A method based on a neural network with potential for global-scale applications. Journal of Geophysical Research, 119, https://doi.org/10.1002/2014JC010355

Sauzède R, Claustre H, Uitz J, Jamet C, Dall'Olmo G, D'Ortenzio F, Gentili B, Poteau A, Schmechtig C (2016) A neural network-based method for merging ocean color and Argo data to extend surface bio-optical properties to depth: Retrieval of the particulate backscattering coefficient. J Geophys Res-Oceans 121, https://doi.org/10.1002/2015JC011408.

Schmechtig Catherine, Claustre Herve, Poteau Antoine, D'Ortenzio Fabrizio (2018). Bio-Argo quality control manual for the Chlorophyll-A concentration. https://doi.org/10.13155/35385

Schmechtig Catherine, Poteau Antoine, Claustre Hervé, D'Ortenzio Fabrizio, Boss Emmanuel (2015). Processing bio-Argo chlorophyll-A concentration at the DAC level. Argo data management. https://doi.org/10.13155/39468

Swart, S., Thomalla, S., and Monteiro, P. (2015), The seasonal cycle of mixed layer dynamics and phytoplankton biomass in the Sub-Antarctic Zone: A high-resolution glider experiment. Journal of Marine Systems, 147, 103-115.

Terrats, L., Claustre, H., Cornec, M., Mangin, A., Neukermans, G. (2020). Detection of coccolithophore blooms with BioGeoChemicalArgo floats. Geophysical Research Letters, 47, e2020GL090559. https://doi.org/10.1029/2020GL090559

Thomalla, S.J., Moutier, W., Ryan-Keogh, T., Gregor, L., and Schütt, J. (2018), An optimized method for correcting fluorescence quenching using optical backscattering on autonomous platforms. Limnology and Oceanography: Methods, 16, 132-144.

Xing, X., Morel, A., Claustre, H., Antoine, D., D'Ortenzio, F., Poteau, A., Mignot, A. (2011). Combined processing and mutual interpretation of radiometry and fluorimetry from autonomous profiling Bio-Argo Floats. The retrieval of Chlorophyll a, Journal of Geophysical Research, 116, C06020, https://doi.org/10.1029/2010JC006899 .

Xing, X., Claustre, H., Blain, S., D'Ortenzio, F., Antoine, D., Ras, J., Guinet, C. (2012). Quenching correction for in vivo chlorophyll fluorescence acquired by autonomous platforms: A case study with instrumented elephant seals in the Kerguelen region (Southern Ocean). Limnology and Oceanography Methods, 10, 483-495.

Xing, X., Briggs, N., Boss, E. & H. Claustre (2018). Improved correction for non-photochemical quenching of in situ chlorophyll fluorescence based on the synchronous irradiance profile, Optic Express, 26(19), 24734-24751. https://doi.org/10.1364/OE.26.024734

6 Annexes

6.1 RT

6.1.1 Tests / updates on DARK CORRECTION

Remove the depth test comparison with MLD

At the ADMT 14, BGC-WORSHOP 2 (2013), Figure 26 was presented to explain why a test was set to exclude from the dark estimation, profiles of floats deployed in strong mixing area, this test was based on the MLD comparison to the depth of the bottom of the profiles :

MLD < Depth_Deepest_Obs - 300 dbar

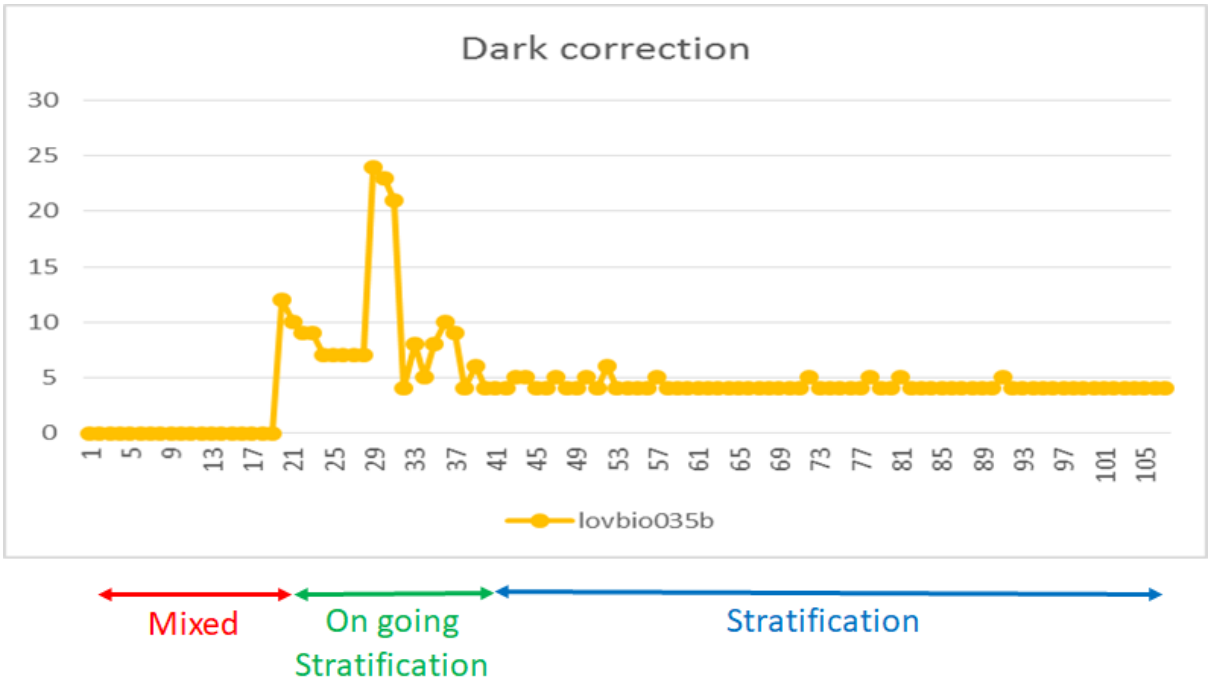

Figure 26: Dark estimation (float lovbio035b, 6901511) presented at ADMT14 (2013) to illustrate that based on the MLD criterion, the dark estimation could only start after profile 20.

While tested over the whole array of floats equipped with fluorometers in 2021, it came out that for about 3200 profiles, the MLD can't be estimated (floats under ice, density threshold (0.03 kg.m-3) not reached...) (Josh Plant comm pers.). Moreover, in his study, this test looks relevant only for the float 6901511 (which was in the initial bunch of Coriolis tested floats for the first version of the QC version). Considering the costs/benefits ratio, it was agreed during the july

2021 BGC-Argo task team meeting to remove this test and to consider the special case of float 6901511 as a DM control.

Remove the dark estimation at depth

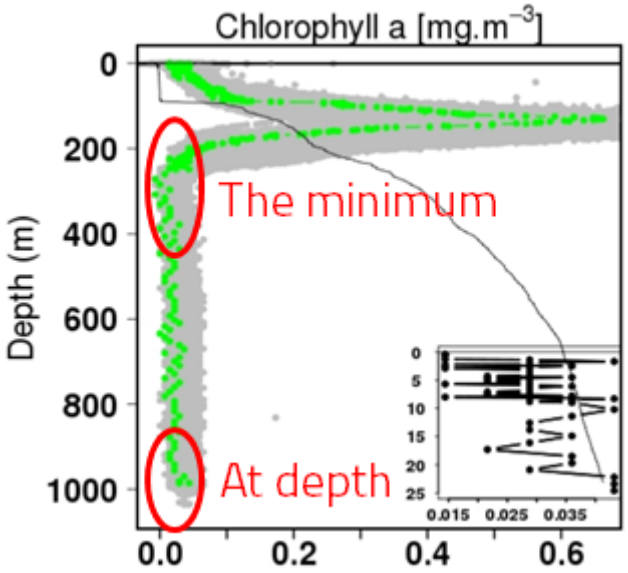

Figure 27 : CHLA profile of float 6901439, highlighting that the minimum value of the CHLA profile is reached just below the DCM and is lower than the value at depth

The initial DARK estimation was performed at depth (https://doi.org/10.13155/35385). This initial dark retrieval leads to an overestimation of the DARK correction which leads to negative value in OMZ (reported by the incois DAC in the indian ocean), in gyres (reported by Coriolis DAC in Atlantic Ocean) as illustrated on Figure 27, particularly just below the DCM and in the Black Sea (reported by the Coriolis DAC).

New Dark value estimation

It was agreed in the BGC-Argo task team in july 2021 to estimate the Dark for the RT adjustment with a median of the minimum of the first five profiles deeper than 900 dbar.

6.1.2 Tests / updates on application of Argo test on CHLA : SPIKE TEST REMOVAL

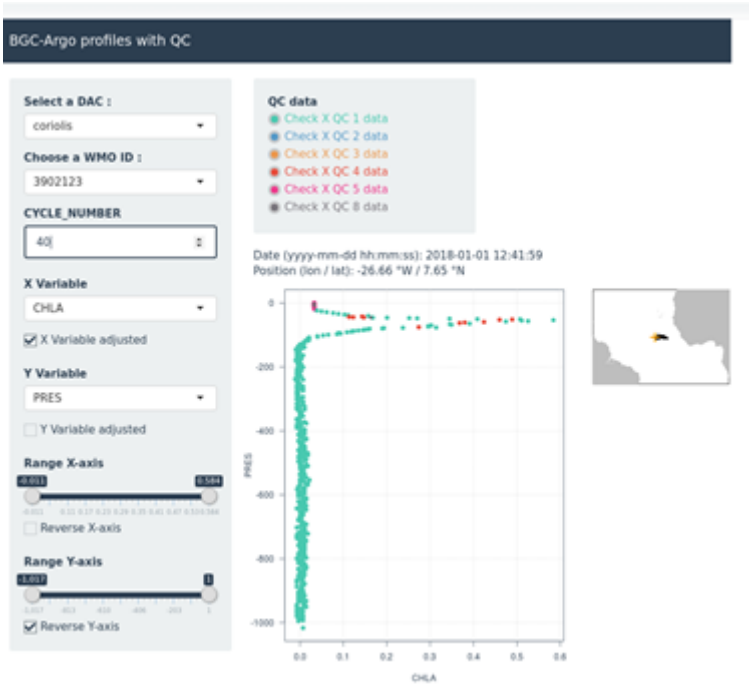

Figure 28 : Profile 40 of the float 3902123 (Atlantic Ocean), red points were levels flagged 4 (Bad)

As illustrated in Figure 28 the initial spike test (https://doi.org/10.13155/35385) is wrongly flagging as QC=4 levels in strong gradient areas.
Despiking correctly the signal for CHLA is tricky and shouldn't be used to assign a QC flag in RT, so the spike detection with QC assignment is moved to the DM procedures as part of the visual quality control while performing DM.

6.1.3 Tests / updates on NPQ CORRECTION

Flowchart of the RT NPQ correction

Xing 2012 flowchart :

zx12=z(FChla=max(median_filtered(FChla(z<0.9*MLD)))

X12(z)=FChla(zx12) if z < zx12
X12(z)=FChla(z) if z > zx12

While testing the whole RTQC and adjustment procedure, it has been decided at the international level to keep the flowchart of the NPQ correction for RT. Associated with the removal of the Argo spike test for CHLA (see previous section), the maximum of the CHLA within 0.9*MLD is obtained after a median filter on CHLA, instead of non filtered but spike free data. Setting up a spike test is really tricky for CHLA, as it extends over several orders of magnitude.

Adding a Sun angle test

The NPQ correction was initially set up for floats programmed to surface at local noon to maximise the chance of obtaining a matchup with ocean color satellites. In recent years, it has been highlighted at the BGC workshop that the floats mission should be adapted to prevent any bias induced by systematic surfacing time at local noon. This change implies that a float can surface at night and as the non photochemical quenching is directly related to light, it is relevant to test the sun angle, before estimating the NPQ correction. On Figure 29, we illustrate that even if the sun angle was not tested in the previous version of the RTQC procedure, Xing et al., 2012 doesn't lead to a bias in the whole data set if applied at night, while with different sun angle test, the scatter plot shape looks similar.

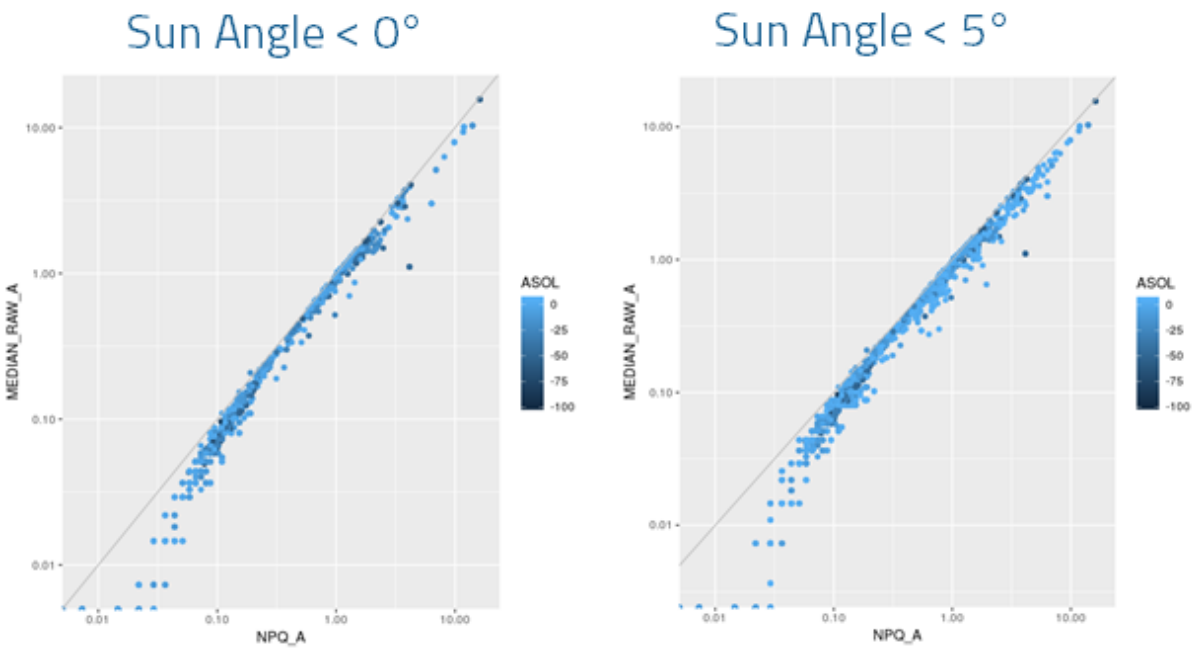

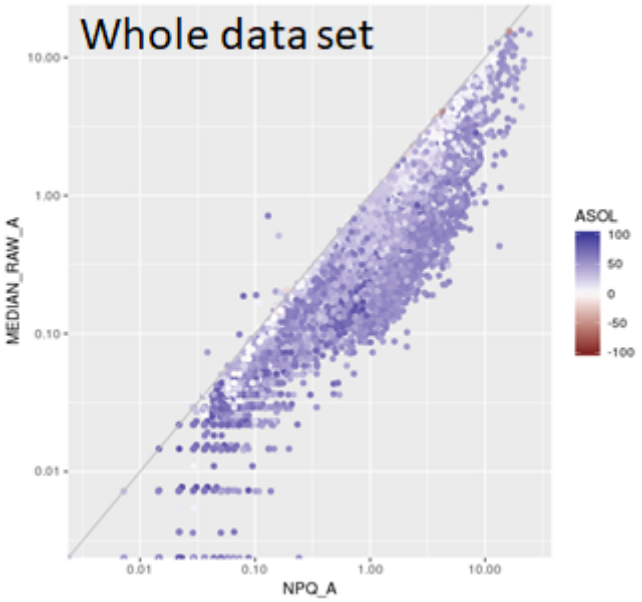

Figure 29 : Illustration of different sun angle tests while comparing the NPQ corrected signal to the raw signal.

6.2 DM

6.2.1 Estimation of slopes for floats equipped with radiometers

The method was widely tested over a large number of floats equipped with radiometers; we present a map (Figure 30) and a table (Table 4) of all the estimated slopes.

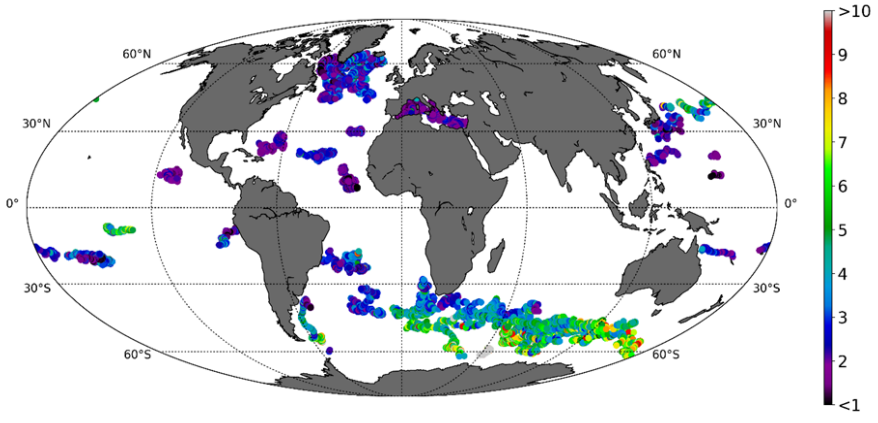

Figure 30 : Slope estimated for Floats equipped with radiometers (DAC: Coriolis, CSIO, BODC)

WMO	DARK	SLOPE_XX (QC 1 or 2)	SD_SLOPE_XX (QC 1 or 2)	AREA
6903197	0.0146	0.5690	0.1227	Adriatic
6901472	0.0216	0.3925	0.0616	North Atlantic
6901525	0.0292	0.4120	0.1521	North Atlantic
6901524	-0.0072	0.3385	0.1816	North Atlantic
6901516	0.0072	0.3530	0.0956	North Atlantic
6901480	0.0000	0.4045	0.1590	North Atlantic
6901485	0.1080	0.4500	0.2357	North Atlantic
6901473	0.0000	0.5610	0.5331	North Atlantic
6901475	0.0000	0.4500	0.0542	North Atlantic
6901474	0.0000	0.4905	0.6586	North Atlantic
6901439	0.0216	0.2920	0.0622	South Atlantic
3902120	0.0365	0.2960	0.1232	South Atlantic
3902121	-0.0365	0.4140	0.2763	South Atlantic
3902122	0.0438	0.6395	0.2103	South Atlantic
3902123	0.0219	0.5960	0.2325	South Atlantic
3902124	0.0288	0.3190	0.1844	South Atlantic
3902125	0.0438	0.3490	0.1434	South Atlantic
6901437	0.0292	0.2820	0.0569	South Atlantic
6901440	-0.0037	0.2200	0.0478	South Atlantic
6901576	0.0075	0.1920	0.0551	South Atlantic
6901582	0.0432	0.2540	0.1104	South Atlantic
6901650	-0.0146	0.1435	0.0586	South Atlantic
6901654	0.0365	0.2700	0.2056	South Atlantic
6901493	-0.0292	0.2060	0.0613	Southern Ocean
6901585	0.0365	0.1590	0.0442	Southern Ocean
6902742	0.0304	0.0650	0.0186	Southern Ocean

6902743	0.0432	0.1200	0.0365	Southern Ocean
6902880	0.0292	0.1340	0.0760	Southern Ocean
6901689	0.0432	0.1630	0.0697	Southern Ocean
6901574	0.0438	0.1440	0.0434	Southern Ocean
6902738	-0.0219	0.2660	0.0852	Southern Ocean
6901579	0.0216	0.1940	0.0599	Southern Ocean
6901584	-0.0146	0.2740	0.1132	Southern Ocean
6902735	0.0504	0.1555	0.0567	Southern Ocean
6902739	0.0146	0.1410	0.0527	Southern Ocean
6902737	0.0365	0.2185	0.0943	Southern Ocean
6901580	0.0000	0.2030	0.0602	Southern Ocean
6902734	-0.0144	0.3240	0.0945	Southern Ocean
6901581	0.0073	0.1950	0.0537	Southern Ocean
6901688	0.0072	0.1430	0.0377	Southern Ocean
6902736	0.0360	0.2150	0.0879	Southern Ocean
6901578	0.0146	0.2380	0.0551	Southern Ocean
6901575	0.0000	0.2060	0.0534	Southern Ocean
6901583	0.0000	0.2340	0.0634	Southern Ocean
6901004	0.0072	0.1520	0.0460	Southern Ocean
6901651	0.0072	0.3315	0.0832	Southern Ocean
6901492	0.0146	0.2850	0.0893	Indian
6903235	0.0000	0.4970	0.6468	Ionian
6901529	-0.0511	0.5955	0.1725	Ionian
6902826	0.0216	0.6465	0.1736	Ionian
6901865	0.0146	0.6170	0.2159	Ionian
6901768	0.0584	0.5330	0.1049	Ionian
6901862	0.0073	0.5390	0.1945	Ionian
6901771	0.0288	0.5295	0.1092	Ionian

6901863	-0.0146	0.4840	0.1079	Ionian
6901510	0.0150	0.5090	0.1147	Ionian
6901765	0.0576	0.4970	0.1046	Ionian
6902828	-0.0073	0.5490	0.7243	Ionian
6901515	-0.0225	0.3330	0.1136	Iceland
6901647	0.0000	0.3415	0.1715	Iceland
6901514	0.0000	0.4065	0.1045	Iceland
6901518	0.0962	0.3650	0.0847	Iceland
6901520	0.0219	0.3520	0.0884	Iceland
6901527	-0.0072	0.3825	0.2002	Iceland
6901519	0.0073	0.2730	0.1004	Iceland
6901522	0.0292	0.3985	0.0369	Labrador
6901486	0.0146	0.4130	0.1606	Labrador
6901489	-0.0292	0.4060	0.2158	Labrador
6901526	0.0288	0.3290	0.0673	Labrador
6901523	0.0219	0.3390	0.1685	Labrador
6901482	-0.0219	0.3270	0.1601	Labrador
6901517	-0.0146	0.3340	0.2294	Labrador
6901646	0.0073	0.3630	0.1864	Labrador
6901484	0.0073	0.3990	0.2365	Labrador
6901481	-0.0072	0.3555	0.4993	Labrador
6901521	0.0288	0.3370	0.1489	Labrador
6901770	0.0360	0.4675	0.0885	Levantin
6902900	0.0288	0.5300	0.1135	Levantin
6901764	0.0144	0.5130	0.0981	Levantin
6901655	0.0146	0.4990	0.1331	Levantin
6901766	-0.0432	0.4780	0.0970	Levantin
6901528	-0.0219	0.4980	0.0957	Levantin

6901773	0.0292	0.5010	0.1175	Levantin
6902733	-0.0073	0.6425	0.1488	Ligurian (NWM)
6902700	0.0225	0.6245	0.1299	Ligurian (NWM)
6902901	-0.0657	0.5520	0.1589	Ligurian (NWM)
6901776	0.0146	0.6440	0.4708	Ligurian (NWM)
6902879	0.0432	0.5420	0.1956	Ligurian (NWM)
6902968	0.0288	0.6290	0.0806	Ligurian (NWM)
6902954	0.0216	0.6860	0.1223	Ligurian (NWM)
6903069	0.0225	0.6225	0.0896	Ligurian (NWM)
6901511	0.0288	0.5735	0.1513	NWM
6901653	0.0576	0.6085	0.1261	NWM
6901861	0.0146	0.5430	0.5794	NWM
6901600	0.0000	0.5960	0.1118	NWM
6901769	0.0365	0.6045	0.1100	NWM
6901032	-0.0073	0.5410	0.2541	NWM
6901512	-0.0146	0.4970	0.1115	NWM
6901649	-0.0584	0.5490	0.1320	NWM
6901513	-0.0219	0.5410	0.0965	NWM
6901648	0.0073	0.5840	0.1536	NWM
6901657	0.0292	0.6675	0.1334	NWM
6902732	0.0073	0.6675	0.4228	NWM
6901496	0.01460	0.6920	0.4301	NWM
6901864	0.0000	0.7015	0.1738	NWM
6902969	0.0432	0.6195	0.1787	NWM
6901774	0.0365	0.5930	0.1252	NWM
6901659	-0.0146	0.3065	0.0728	Pacific
6901660	0.0144	0.3140	0.0727	Pacific
6901687	0.038	0.6165	0.3032	Pacific

6902701	0.0000	0.3270	0.1530	Pacific
6902827	0.0584	0.4735	0.2222	Pacific
6902905	0.0219	0.2000	0.0507	Pacific
6902906	0.0000	0.2130	0.0815	Pacific
6902907	0.0438	0.2220	0.0636	Pacific
6902908	0.0216	0.2590	0.0933	Pacific
6902909	0.0073			Pacific
6901656	0.0142	0.4200	0.1053	Pacific
6901658	0.0284	0.4250	0.0783	Pacific
6901767	0.0720	0.6390	0.1326	Thyrenian
6901491	0.0073	0.5580	0.1394	Thyrenian
6902903	0.0000	0.6370	0.1371	Thyrenian
6901490	0.0216	0.4830	0.0473	Thyrenian
6901483	0.0000	0.5345	0.1063	Thyrenian

Table 4 : All slope estimation for Coriolis floats equipped with radiometer.

6.2.2 Estimation of slopes for floats not equipped with radiometers

The method was widely tested over a large number of floats not equipped with radiometers; we present a map (Figure 31) of all the estimated slopes.

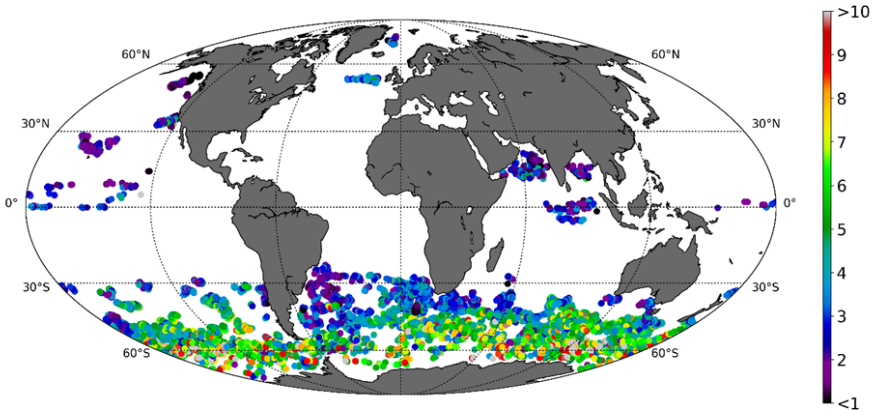

Figure 31 : Slope estimated for Floats not equipped with radiometers (DAC: Aoml, INCOIS)

6.2.3 RMS with satellite products in RT and in DM

A global rough study (without a visual QC, but accounting for STEP 1: Dark estimation, STEP2 : Non Photochemical Quenching correction and STEP3: Slope estimation) was performed on 197 Aoml floats and 116 coriolis floats equipped with fluorometers. To assess the improvement of the DM procedures, we estimate the RMS compared to satellite products for both RT and DM. We can see on Figure 32 that the DM decreases dramatically the RMS for the AOML floats compared to RT. A large number of AOML floats were deployed in the Southern Ocean where the slope estimated strongly differs from the mean slope applied in RT (Roesler et al., 2017). For these floats, the correction leads to a huge improvement of the DModed parameter. For Coriolis floats, the improvement is not as spectacular, but nevertheless present, while a large number of floats were deployed in the Mediterranean Sea, where the slope estimated is very close to the RT mean slope.

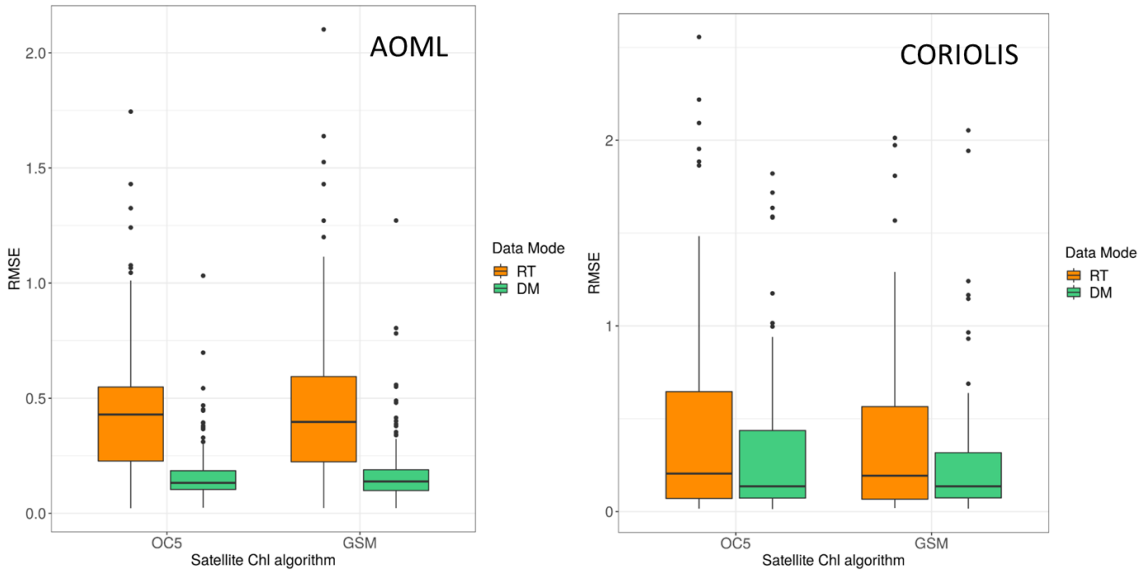

Figure 32 : RMSE between CHLA_ADJUSTED from floats at surface and Chla product for two algorithms (OC5, GSM from satellite matchup (DAC: Aoml, Coriolis)